Achievable Rates of Iterative MIMO Receivers over Interference Channels

Farrokh Etezadi

A thesis

in

The Department

of

Electrical and Computer Engineering

Presented in Partial Fulfillment of the Requirements

For the Degree of Master of Applied Science

Concordia University

Montréal, Québec, Canada

January 2010

Your file Votre référence
ISBN: 978-0-494-67097-2
Our file Notre référence
ISBN: 978-0-494-67097-2

Abstract

Achievable Rates of Iterative MIMO Receivers over Interference Channels

Farrokh Etezadi

In this thesis, we study the achievable rates of some interference communication schemes when iterative interference-cancellation (IC) is applied. We assume multiple-input multiple-output (MIMO) communication employing iterative receivers with linear front-ends which involves two modules concatenated serially and cooperating iteratively; a linear combiner based on minimum-mean-square-error (MMSE) detection or maximal-ratio-combining (MRC) and a SISO decoder. We investigate the achievable rates of this receiver when the transmitted signal is Gaussian-distributed with hypothetical erasure-type feedback from the decoder to the combiner and a more practical case with large-size QAM constellations with log-likelihood-ratios (LLRs) being exchanged between the receiver's modules. The achievable rate is approximated by the area below the EXIT curve of the linear FE receiver. Some properties have been observed and mathematically been proved about the iterative MIMO receivers with linear front-end.

Inspired by the meaningful relationship between achievable rate of MIMO-MMSE and MIMO systems, the general relation between the single-user and multi-user uplink MIMO capacity is explained which it is simply the Chain rule of information theory. As a result, another simple proof for the capacity of BICM system is presented.

Furthermore a new scheme of CFO-corrupted OFDM with Alamouti coding in two-relay communication system is introduced and the effect of interference caused by CFO on the communication performance is investigated. Different scenarios, including different CFO differences, non-iterative and iterative receiver, relay selection, are investigated and compared. As a suitable support for the results, the practical transmission with well-known turbo code is implemented and the bit-error-rate (BER) results are discussed.

Dedicated to my dearest mother, father, and sister ...

Acknowledgments

First of all, my sincere appreciation goes to my academic supervisors Dr. Leszek Szczecinski and Dr. Ali Ghrayeb who have offered me invaluable support, constructive guidance and helpful discussion throughout my thesis research. I am grateful for their patience and kindness in answering my questions and revising my submitted reports. Without their continuous encouragement and stimulating suggestions I would not have completed my thesis.

I would like to thank the committee members Dr. M. R. Soleymani, Dr. Y. Zeng and Dr. A. Aghdam. Their comments make the presentation of this thesis more clear.

I want to thank all the people who help me throughout my study at Concordia University. Finally, I would like to thank my parents for their love, trust and encouragement throughout all the two years. Without their support, it would have been impossible for me to accomplish what I have accomplished.

Contents

List of Figures

Chapter 1

Introduction

1.1 Motivation

In telecommunication, interference is anything that disturbs, alters or modifies the signal while passing through a communication channel between the source and the destination. Although there are various kinds of interferences, which are mostly classified based on their generating sources in different communication systems, all affect the performance of the communication and need to be mitigated through the receivers' process. Inter-symbol interference, electromagnetic interference, co-channel interference (crosstalk), multi-user interference, inter-carrier interferences, etc. are some common interferences which affect the communication performance in different transmission schemes. In modern digital communication,

high-tech receivers employ advance interference cancellation algorithms to attenuate this damaging effect. However, it is not always possible for the receivers to completely eliminate the interference. Iterative receivers, like turbo receivers, provide the possibility of iteratively reducing the interference level and getting as much information as possible from the received signal. Despite the fact that iterative processes have been studied extensively and developed for different kinds of iterative interference cancellation, like turbo decoder, turbo equalizations, turbo synchronization and so on, there is no general analytical framework for evaluating the performance of such systems. The main motivation of this thesis is to answer the following question that: "How much can an iterative receiver mitigate the interference?". The importance of the answer to this question is obvious as it clarifies the ultimate performance limit of the iterative receivers in different communication systems.

1.2 Problem Statement

A very useful measure of communication performance is the mutual information between the transmitted and received signals which leads to insights about the maximum achievable rate of the system, i.e. the maximum rate of information which can be transmitted through the channel with diminishing probability of error, while employing optimum codes. In this thesis, we always consider the

mutual information as a performance criterion of the underlying communication system.

Perhaps multiple-input-multiple-output (MIMO) systems are the most general and well-known example of interference suffering communication systems. MIMO systems are typically equipped with N_t transmit and N_r receive antennas, which communicate with each other through a MIMO channel, i.e. $\mathbf{H}$. In the receiver side, while detecting the symbol transmitted by the ith transmit antenna, in addition to the independent additive white Gaussian noise (AWGN) noise caused by unpredictable sources in the antennas (for example thermal noise), some interference caused by the symbols coming from the other transmit antennas appear and influence the detection process. Optimum MIMO receivers consider the whole arriving signals through all the receiver antennas and perform maximum likelihood (ML) detection to estimate the transmitted signals.

Nevertheless, increasing the number of transmit antennas leads to a practical problem while implementing ML sequence detection. Since this may be unrealistically complex, for practical reasons, the detection is decoupled into two stages: first the transmitted coded symbols/bits are estimated, and next are used for decoding (assuming some sort of channel coding is employed). The suboptimality of this approach may be compensated to a certain extent through the so-called turbo processing where the detector and the decoder iteratively exchange information on the coded bits. The idea of such turbo MIMO receivers

is an extension of the technique invented for decoding concatenated codes (e.g. turbo codes).

In fact, turbo processing may be theoretically equivalent to optimal sequence detection, that is, using the iterative receiver we might transmit with the maximum achievable rate. This is true if the information exchanged about the bits/symbols is equivalent to the transmission over the erasure channel and the devices of the turbo receiver operate in an optimal way (i.e., implement the ML detection). However, such a condition may be difficult to encounter in practice. First of all, the erasure-type information is not produced by the state-of-the-art decoders/detectors. That is, such decoders calculate reliability measures (the so-called soft information) in the form of logarithmic likelihood ratios (LLRs). This is in particular due to the popularity of binary channel encoders and the soft-input soft-output (SISO) decoder. Secondly, the maximum likelihood detection may be impractical if the search space becomes too large, as is the case in MIMO systems with many transmit antennas and high-order signal constellations. In such a case, sub-optimal, e.g., linear front-end detectors are an interesting alternative.

One interesting problem, which we investigate in this thesis, is finding the maximum theoretical achievable transmission rates if such turbo processing is applied, particularly when sub-optimal detectors are used.

Another example of interference channels is the scenario of inter-carrier interference that is experienced in carrier frequency offset (CFO)-corrupted orthogonal frequency division multiplexing (OFDM) systems employing space-frequency coding over relay channels. In this case one transmitter tries to send information bits to one receiver through some relay antennas. CFO causes inter-carrier interference which theoretically can be completely mitigated at the receiver in point-to-point OFDM communication systems. However, using more than one relay channel introduces different independent CFOs. Consequently, the receiver cannot mitigate the CFO effect of both relay channels at the same time. Indeed, correcting the frequency offset for one channel would cause more interference for the other channels. This is an example of interference suffering communication. The performance of the receiver with and without iterative detection/decoding is a very interesting problem, which we address in this thesis.

1.3 Contributions

The main contributions of the thesis are listed as follows.

- The performance of MIMO receivers employing linear front-ends, in the sense of achievable sum rate, for non-iterative and iterative schemes are derived. The iterative receiver in this setting involves two modules concatenated serially and cooperating iteratively. The inner module is merely

a linear combiner based on minimum mean square error (MMSE) detection or maximal ratio combining (MRC). The outer module is assumed to be a SISO.

- It is shown that, at low and high SNRs, the rates achievable by iterative and non-iterative MIMO receivers based on MMSE are the same. In other words, although the introduced iterative interference cancellation increases the maximum achievable rates by the receiver, it does not improve the detection performance in the receiver in the low and high SNR regimes

- A very useful representation of single-user MIMO capacity is investigated which relates this capacity to the multi-user one. Capacity of two popular transmission schemes (MIMO-MMSE and BICM) are shown as specific applications of such single-user multi-user model.

- The impact of CFO on the performance of OFDM transmission employing space-frequency coding over relay channels is studied. The performance of the receiver in such systems when it tries to iteratively mitigate the interference (caused by multiple CFOs) is studied and the achievable rates for different relaying schemes are compared.

1.4 Thesis Outline

In Chapter 2, background material, which should enable the reader to follow the rest of the thesis, is presented. The basics of MIMO systems and their capacity analysis, basic concepts of the iterative processing in the receivers and other basic model like OFDM systems are explained.

In Chapter 3, the achievable rates of iterative MIMO receivers with linear front-ends are discussed in detail and several numerical examples are presented.

In Chapter 4, the concept of single-user and multi-user capacities and the relation between them based on the so-called Chain rule of information theory is introduced. We consider the MIMO-MMSE and BICM systems' capacities as special cases.

In Chapter 5, the two relay communication exploiting the Alamouti space-frequency coding scheme for OFDM systems is introduced and the effect of CFO on the communication performance is studied in detail.

In Chapter 6, conclusions are made and directions for future work are suggested.

Chapter 2

Literature Review

In this chapter, we discuss the background of various concepts of wireless communications, which is needed to understand the material presented in the subsequent chapters. In particular, we touch on MIMO systems in terms of capacity, space-time codes, diversity versus multiplexing trade-off. We also consider the concepts of iterative receivers including extrinsic information transfer (EXIT) charts and some of its properties, iterative MIMO and iterative synchronizations. Finally, the basic ideas and a very simple model of OFDM communications are presented.

2.1 MIMO

2.1.1 Capacity

Basic interest in sending as much information as possible from one point to another, which is one of the main aims of the research efforts in telecommunication, has motivated the developments of low complexity power, bandwidth efficient communication systems during the past decades. One important development of such systems appeared, while exploiting multiple transmit and receive antennas in MIMO systems, which enabled much higher rates using space diversity compared to single-input single-output systems. Works by Telatar [1], and Foschini and Gans [2] explained the improvements in spectral efficiency while using multiple antenna systems in rich scattering and well-tracked MIMO channels. It is shown that, in such channel condition, a single user MIMO system with N_t transmit and N_r receive antennas can approximately achieve the capacity of $\min\{N_t, N_r\}$ separate channels. Thus, capacity scales linearly with $\min\{N_t, N_r\}$ relative to a system with just one transmit and one receive antenna.

By channel capacity we mean the Shannon capacity [3]. The Shannon capacity, defined as maximum mutual information, through a single-input single-output time-invariant channel, corresponds to the maximum transmission rate achievable with an arbitrary small probability of error. Specifically, Assuming the general

MIMO transmission as

$$\mathbf{y} = \mathbf{H}\mathbf{x} + \mathbf{n}, \tag{1}$$

where $\mathbf{x}$ and $\mathbf{y}$ are vectors of the input and output symbols, respectively, and $\mathbf{n}$ is a vector of white Gaussian noise (AWGN). The channel capacity is given by the maximum mutual information between the input and the output of the MIMO channel as

$$\mathrm{C} = \max_{p(\mathbf{x})} I(\mathbf{x};\mathbf{y}) = \max_{p(\mathbf{x})} \left[\mathbf{H}(\mathbf{y}) - \mathbf{H}(\mathbf{y}|\mathbf{x})\right], \tag{2}$$

where $\mathbf{H}(.)$ represents the entropy function and maximization is done over all input probability density functions (PDFs). While the entropy of the noise does not depend on the input vector, the above maximization problem reduces to entropy maximization of the output vector, i.e., $I(\mathbf{y})$, which is maximized when $\mathbf{y}$ is a zero-mean circularly-symmetric complex Gaussian (ZMCSCG) random vector. This requires the input signal, $\mathbf{x}$, to be ZMCSCG and thus

$$\mathrm{C} = \log_2 \det\left[I_{N_\mathrm{r}} + \mathbf{H}\mathrm{R}_\mathbf{x}\mathbf{H}^\dagger\right], \tag{3}$$

where

$$\mathrm{R}_\mathbf{x} = \mathbb{E}\left\{\mathbf{x}\mathbf{x}^\dagger\right\}, \tag{4}$$

is the covariance matrix of the random vector $\mathbf{x}$ and $(.)^\dagger$ represents the conjugate transpose operation.

When the transmitter has no information about the channel, naturally, it transmits through the transmit antennas with equal powers, i.e. $R_{\mathbf{x}} = \frac{\rho}{N_t} I$. When both of the transmitter and receiver know the channel state information (CSI), the channel capacity is derived using well-known water-filling strategy.

For time-variant channels, e.g., fading schemes, different capacities can be defined, depending on what is known about the instantaneous CSI at the transmitter and/or receiver. Specifically, the channel capacity is usually characterized by the ergodic and the outage capacities.

The ergodic capacity defines the maximum average rate under an adaptive transmission strategy averaged over all channel states (long-term average). The outage capacity defines the maximum rate that can be maintained in *all* channel states with some probability of outage (no data transmission). Here in this thesis we talk about the ergodic channel capacity most of the time, except in Chapter 4 where the outage capacities for special cases are computed as they provide more insight about the practical transmission schemes.

Although assuming Gaussian distributed input signals gives some insights about the transmission rate, symbols in real practical systems belong to constellations which are not Gaussian. Constellation-constrained capacity provides information about the maximum achievable rates in such more practical cases.

2.1.2 Spatial Multiplexing and Diversity

Two options can be considered to improve the communication performance utilizing multiple antenna systems. First, achieving the capacity gain by decomposing the MIMO channel into several parallel channels and sending data streams through those. This introduces the capacity gain referred to as multiplexing gain and is achieved by exploiting the spatial diversity in multiple antennas. The SNR associated for each sub-channel depends on the singular values of the channel, **H**. These sub-channels perform reliably only for low data rates. Second, using strategies like beamforming coherently combines the MIMO channel gains to achieve a robust channel between transmitter and receiver with high diversity gain. Thus, a natural trade-off between the multiplexing gain and diversity gain appears in multiple antenna systems [4]. Commonly, a transmission scheme is said to achieve multiplexing gain r and diversity gain d if the data rate (bps) per unit Hertz $R(\mathrm{SNR})$ and probability of error $P_e(\mathrm{SNR})$ as functions of SNR satisfy [5]

$$\lim_{\log_2(\mathrm{SNR})\to\infty} \frac{R(\mathrm{SNR})}{\log_2(\mathrm{SNR})} = r, \tag{5}$$

and

$$\lim_{\log_2(\mathrm{SNR})\to\infty} \frac{\log_2 P_e(\mathrm{SNR})}{\log_2(\mathrm{SNR})} = -d. \tag{6}$$

2.1.3 Space-Time Modulation and Coding

As mentioned before, in multiple antenna systems, at each transmission time, a vector of symbols is transmitted by the transmit antennas. Thus, the signal design extends over both space (via multiple antennas) and time (via multiple symbol times), it is typically refereed to space-time coding. A space-time block code (STBC) is usually described by a matrix whose rows and columns represent the signals being transmitted through different transmit antennas and different transmitting time slots, respectively. We first describe the Alamouti scheme [6] as a simple way of obtaining transmit diversity for the case of two transmit antennas. Alamouti block code is as follows:

$$\mathrm{X} = \begin{bmatrix} x_1 & x_2 \\ -x_2^* & x_1^* \end{bmatrix}, \tag{7}$$

which means at the first time slot x_1 and x_2 are transmitted by the first and second antennas, respectively, and in the second time slot $-x_2^*$ and x_1^* are transmitted by the first and second antennas, respectively. Since the two symbols are transmitted in two time slots, the overall transmission rate is one symbol per channel use.

Denote $h_i, i = 1, 2$ as the fading coefficient between the i^{th} transmit antenna and the receive antenna (assuming a single receive antenna). Assume the fading coefficients are constant across the corresponding two consecutive time slots.

Then the received signal at the first and second time slot can be represented as

$$\begin{aligned} y_1 &= h_1 x_1 + h_2 x_2 + n_1, \\ y_2 &= -h_1 x_2^* + h_2 x_1^* + n_2, \end{aligned}$$

respectively, where n_1 and n_2 are independent noise samples added by the receive antenna in each time slot. In order to extract x_1 and x_2, the received signal y_1 and y_2 are combined according to

$$\begin{aligned} \tilde{x}_1 &= h_1^* y_1 + h_2 y_2^* \\ &= \left(|h_1|^2 + |h_2|^2\right) x_1 + h_1^* n_1 + h_2 n_2^* \end{aligned}$$

$$\begin{aligned} \tilde{x}_2 &= h_2^* y_1 - h_1 y_2^* \\ &= \left(|h_1|^2 + |h_2|^2\right) x_2 + h_2^* n_1 - h_1 n_2^*. \end{aligned}$$

The decision statistics $\tilde{x}_1$ and $\tilde{x}_2$ are then passed to the ML detector to determine the most likely transmitted symbols.

The full diversity of the MIMO system, which is two for the case of two transmit and one receive antennas can be obtained with the use of the Alamouti scheme. For higher number of antennas, the transmit diversity can be extended using general space-time block codes based on the theory of orthogonal designs [7]. STBCs, if properly designed, in addition to providing full spatial diversity, can be decoded efficiently using linear processing at the receiver.

Another basic coding scheme for exploiting space diversity in MIMO systems is space-time trellis coding (STTC) which is very similar to the idea of convolutional coding which provides some coding advantages over the approach of STBC. However, the decoding of STTCs is more involved compared to that of STBCs.

2.1.4 Bell Labs Layered Space Time (BLAST) Coding

In order to achieve full diversity in MIMO systems, an encoded bit stream must be transmitted over all N_t transmit antennas. This can be done through a serial encoding, illustrated in Figure 1, where information bits are first encoded, interleaved and mapped to a constellation and then demultiplexed onto the different antennas. If the codeword is sufficiently long, it can be transmitted through all N_t transmit antennas and received by N_r receive antennas and achieve the full diversity order of $N_t N_r$. Decoding complexity grows exponentially with this codeword length. This high level of complexity makes serial encoding impractical.

Vertical-BLAST (VBLAST) [8] is a simple way of achieving spatial multiplexing (Figure 2). In this scheme, information data, is first demultiplexed and each of the resulting sub-streams is passed through a single-input single-output encoder, interleaved, mapped to a signal constellation point, and transmitted over its corresponding transmit antenna. The diversity order in this system reaches

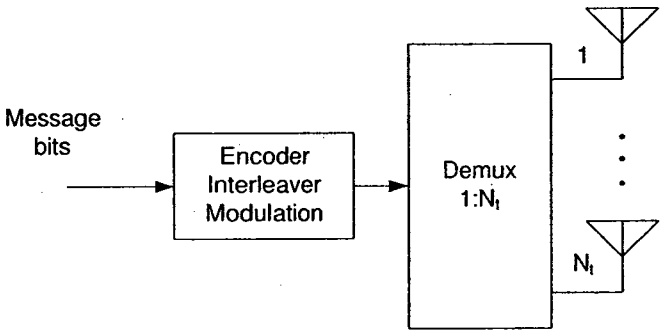

Figure 1: Spatial Multiplexing with Serial Encoding.

at most the number of receive antennas (N_r) [5]. More specifically, when channel encoding is involved, the VBLAT scheme changes into two possible schemes, i.e. HBLAST and SCBLAST, as shown in the Figures 3 and 4 [9]. Generally, VBLAST has a simple encoding complexity, however ML decoding still requires joint detection of the codewords from all transmit antennas and seems to be computationally complex even for small number of transmit antennas. This complexity grows exponentially in the number of transmit antennas and the number of states of the channel code.

Other less complex but suboptimal approaches are commonly used for detecting BLAST signals, including the detection algorithms based on the zero forcing (ZF) and the MMSE criteria. The receiver complexity can be significantly reduced through the use of symbol interference cancellation (IC). In this

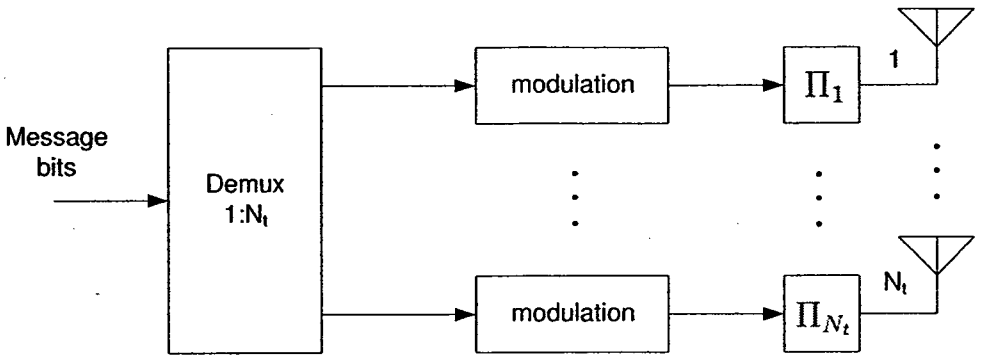

Figure 2: VBLAST encoder structure.

method, the received streams are sorted in terms of their received SNR. An estimate about the symbol with the highest SNR is made while treating all other symbols as noise. This estimated symbol is subtracted out and the next highest SNR symbols goes to estimation process. This method repeats till all transmitted symbols are estimated. After canceling out interfering symbols, the coded substream associated with each transmit antenna can be individually decoded. In Chapter 3, we consider MIMO receivers with linear front-ends, more specifically based on MMSE and MRC, and we talk about the achievable sum rate of such receivers employing IC through iterative receiving process.

The diagonal BLAST (DBLAST) [10] combines two techniques of serial and vertical encoding to achieve both benefits of VBLAST and diversity benefits of serial encoding. The DBLST encoder structure is shown in Figure 5. In D-BLAST, the data stream is first horizontally encoded. However, rather than transmitting the independent codewords on separate antennas, the codeword symbols

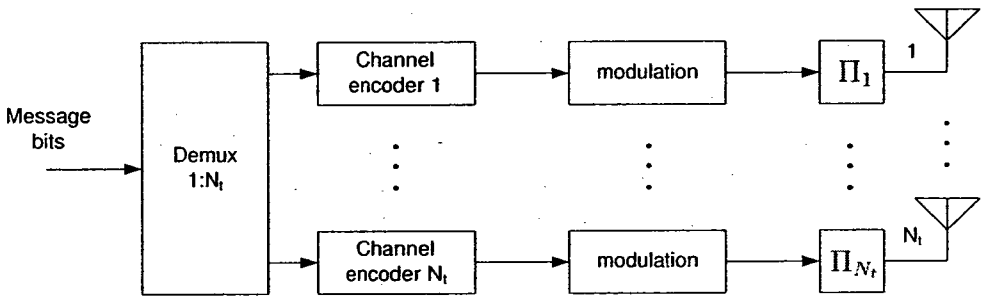

Figure 3: HBLAST encoder structure.

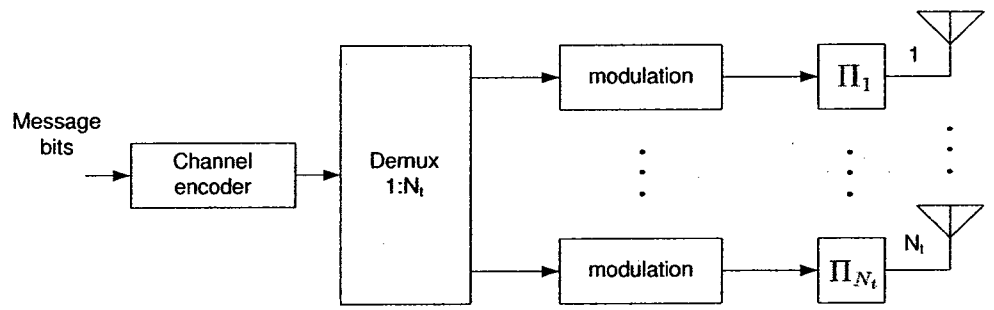

Figure 4: SCBLAST encoder structure.

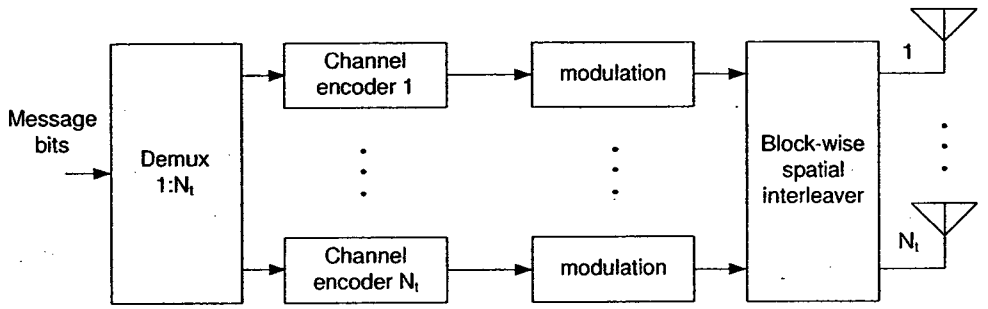

Figure 5: DBLAST encoder structure.

are rotated across antennas, so that a codeword is spread over all N_t antennas. The motivation behind this transmission scheme is to introduce some additional spatial diversity that VBLAST scheme lacks.

2.2 Iterative Receivers

Concatenated codes, whose general idea first introduced by Forney [11] and practical system developed by Odenwalder [12] , involved concatenating two single codes in a serial fashion; the inner code is a convolutional code and the outer code is a high-rate Reed-Solomon (RS) code with powerful error correcting capability. The performance improvements achieved by this concatenated coding scheme motivated further developments in this area. In the decoding process, the receiver elements were modified to be able to utilize some reliability information provided by the other elements to perform better detection and, in addition to

hard decision, provide some reliability information for the other receiver's elements.

The discovery of turbo codes by Berrou et al. [13] marks one of the most important breakthroughs in the history of coding theory. A typical turbo code comprises parallel concatenation of two convolutional codes separated by an interleaver, and is decoded using iterative decoding techniques. Turbo codes became very important mainly because for their exceptional performance for very low SNRs. Inspired by turbo codes, a new concatenation scheme was proposed by Benedetto et al. [14] which involves the serial concatenation of two convolutional codes separated by an interleaver and decoded using iterative techniques. Another major development in capacity achieving coding has been low-density parity check (LDPC) codes [15], [16]. They achieve near capacity performance, and they are decoded via the so called message passing or belief propagation algorithm.

The turbo principle, originally invented for decoding of concatenated codes, can be applied for many decoding and detection problems such as parallel or serial concatenation (PCCC and SCCC respectively), equalization [17], coded modulation, multiuser detection [18], MIMO detection [19], joint source and channel decoding, LDPC decoding and others. In many cases, the turbo processing can be shown as a serial concatenated encoder and decoder as Figure 6. The main point at the receiver is that there are two SISO decoders at the receiver which accept and deliver probabilities or soft values. The extrinsic part of the soft-output of

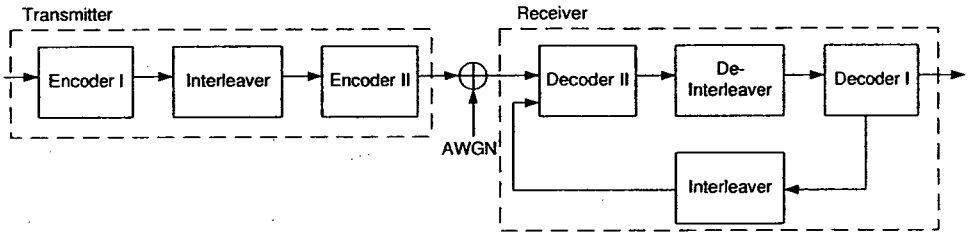

Figure 6: A serial concatenated system with iterative detection/decoding.

one decoder is passed on to the other decoder to be used as a priori input. In other words, the two decoders in the receiver exchange information between each other in order to get more information about the transmitted signal.

2.2.1 EXIT Charts

Ten Brink [20] introduced extrinsic information transfer (EXIT) chart as a very useful method to study the convergence behavior of turbo receivers. The idea behind the EXIT chart is to derive the diagram which relates the mutual information between the transmitted signal and the soft-input of a decoder to the mutual information between transmitted signal and the soft-output of that decoder. In other words, the EXIT chart of each decoder element shows how much information it would provide about the transmitted bits by knowing partial information about these bits. The output of one decoder provides a priori information as the input of the next receiver element. It was shown in [20] that if the EXIT charts of two decoder elements are plotted as the same chart, the iteration process

can be well approximated by trajectories in the charts.

In turbo receivers, the information exchanged between the decoder elements is normally the LLRs of the bit defined as

$$L(u) = \ln \frac{p(u=+1)}{p(u=-1)}. \tag{8}$$

Consequently, we can write

$$P(u=\pm 1) = \frac{e^{\pm L(u)/2}}{e^{L(u)/2} + e^{-L(u)/2}}, \tag{9}$$

which suggests that the LLR, as a random variable itself, is the only parameter which fully describes the probability distribution of the information bits. Analyzing the PDFs of these random variables (i.e. LLRs) allows predicting the behavior of the decoding algorithm, but this is, unfortunately, extremely difficult for most system configurations. A substantial simplification is to observe only a single parameter of these PDFs such as the mutual information between LLRs and transmitted bits, like the EXIT charts. Characterizing the probability distribution of the LLRs is much simpler if the PDF is both symmetric and consistent [21].

While deriving the EXIT charts for iterative receivers and investigating convergence behavior, it is very useful to assume that the extrinsic information provided by the other receiver's element(s) are coming from another channel called *extrinsic channel* or *a priori channel* [22]. This is a valid assumption while considering sufficiently large interleaving. Various models can be assumed for this

extrinsic channel, e.g. Gaussian channel, binary erasure channel (BEC), binary symmetric channel (BSC), etc.

The Area Property of EXIT Charts

Ashikhmin et al. [22] introduced very useful properties of EXIT charts which relates the achievable rates to the EXIT function. More precisely, they showed that, considering the BEC extrinsic channel, the area under the EXIT chart represents the achievable rate or the code rate (for EXIT chart of outer or inner decoder in serially concatenated code, respectively). This so-called area property was studied later in more detail and generalized for other types of extrinsic channels, specially for LDPC codes in [23].

One of the interesting advantages of these kinds of area properties is changing the traditional decoder design problem to a curve fitting problem. It means that, as the area under the EXIT chart for inner decoder represents the maximum achievable rate, the optimum outer decoder is the one whose EXIT curve fits the EXIT curve of the inner decoder. Although these are the results achieved for BEC channels, it has been used as a good approximation for other more practical types of iterative receivers [24].

2.2.2 Iterative MIMO Receivers

In MIMO receivers, specially when the number of transmit antennas as well as the size of the signal constellations grows, implementation of optimum detection (ML) becomes very hard and not practical. As such, the detection process is divided into two separate steps: First, the symbols are estimated and then the estimated symbols are provided to the outer decoder to eliminate the redundancy of the channel code and extract the information about the transmitted bits. Still, the complexity of the ML detection is High. Thus, employing linear combiners based on MMSE, MRC, ZF appears to be a good alternative.

The performance of MIMO receivers with linear front ends (FE) is a very interesting topic. There are some recent papers talking about the achievable rates of such receivers (like MIMO-MMSE [25]) on different fading channels. The idea of iterative receiver can be applied in this case. That is, the soft information about the transmitted bits (and thus about transmitted symbols) coming from the outer decoder (turbo decoder) is used in the linear combing and symbol detection processes. Investigating the performance of such systems, from the achievable rate point of view, is treated in Chapter 3 of this thesis.

2.2.3 Synchronization

Synchronization is the processing of the received analog signal to be correctly aligned in the sense of sampling time, phase and frequency, in order to improve the detection process. The synchronization methods can be divided into non-data-aide (NDA) or data-aided (DA). The DA techniques rely on the presence of pilot symbols in the data frame and may lead to unacceptable loss in terms of power and spectral efficiency. On the other hand, NDA synchronization algorithms extract some statistical information about the transmitted signal and may lead to very poor results at low SNR. As an alternative, some other methods take advantages of the *coding gain* for synchronization purposes and are known as code-aided (CA) methods [26].

Simple Model

In a very simple bandpass data transmission scheme, a bit stream $\mathbf{u}^\dagger = [u_1, u_2, ..., u_L]$ is transformed in two mapping process, first a channel encoder encodes the data bits and coded data $\mathbf{c}^\dagger = [c_1, c_2, ..., c_N]$ is generated. Then coded data is mapped to a symbol vector $\mathbf{a}^\dagger = [a_1, a_2, ..., a_K]$ which, in order to be sent through physical medium (free space, optic fiber, wire line,...), is modulated to a bandpass frequency and the analog signal is generated. The reverse operation in the receiver is demodulating and consists in the transformation of the received analog signal to discrete-time samples which can be further processed by some numerical

algorithms. The responsibility of the receiver is to estimate the transmitted bit stream **u** knowing the received signal. This estimation is performed well while fully synchronized signal is fed to the estimator.

For a very simple transmission channel modeled as Gaussian, the received baseband signal is in the following form

$$\mathrm{r}(t) = A\sum_{k=1}^{K} a_k g(kt - T - \tau)e^{j(2\pi\nu t+\vartheta)} + n(t), \tag{10}$$

where T is the symbol period, $g(t)$ is an analog pulse, $n(t)$ is an additive Gaussian noise with (known) power spectral density N_0, and A, τ, ν, ϑ are unknown synchronization/channel parameters: amplitude, delay, CFO, and carrier phase offset, respectively. At the receiver, one has to apply some processing to the observed signal $r(t)$ in order to recover the transmitted message u. First, the signal in 10 is sampled at rate $1/T_s$, and the relevant signal samples are collected into the observation vector **r**. From this vector, one then computes an estimate, say $\tilde{\mathbf{u}}$, of the information bits **u**.

In the traditional non-iterative receivers, a separate synchronizer tries to estimate the synchronization vector, $\mathrm{b} = [A, \tau, \nu, \vartheta]$ in this case, and compensate the effect of this synchronization parameters on the received signal to provide a cleaner signal for detection.

Iterative Synchronization

The introduction of turbo codes motivated the idea of exploiting the so-called soft information provided by the SISO decoder in the synchronization process in order to reduce the synchronization imperfections in an iterative manner. Since then, many techniques have been developed for turbo equalization and synchronization.

The basic idea of turbo synchronization is to iteratively improve the estimates of synchronization parameters employing the soft information about the bits coming out from the decoder. Turbo synchronization are commonly based on three methods; expectation maximization (EM) algorithm, gradient method and sum product algorithm (SP) [26].

The EM method is an iterative method to solve ML problems and when well designed can reduce the complexity of the ML problem very much by dividing the solution into two steps (E-step, M-step) which repeat iteratively till solving the problem [27]. The gradient method works based on the fact that iteratively taking steps in the direction of the gradient of a function results in reaching the optimum solution (in the presence of some convergence conditions). The SP algorithm is based on representing the marginalization problem by a graph and it can be shown that message passing and sum product algorithm converges to a marginalized solution for the graphs without cycles [28], [29].

2.3 OFDM Communication

Orthogonal frequency division multiplexing (OFDM) is an efficient transmission scheme over fading channels. It has been adopted in many wireless communication standards including WiFi, WiMax, and LTE [30], [31]. In this scheme information is modulated into several small frequency bands, called subcarriers, which are orthogonal in the frequency domain. The implementation of the OFDM modulator and demodulator is achieved via using fast Fourier transform (FFT) and inverse FFT (IFFT) algorithms which can be implemented with an acceptable computational complexity.

The main advantage of OFDM is that it allows transmission over highly frequency-selective channels at a low receiver implementation cost. In particular, costly equalizers needed in single-carrier systems are dramatically simplified or even avoided in the case that differential modulation schemes are used. OFDM transmission does not suffer from strict time-synchronization requirements but its well-known disadvantage is sensitivity to frequency-synchronization errors, i.e. CFO.

2.3.1 Simple Model

Transmitter

Here we explain an OFDM system using IFFT of size N for modulation. Each OFDM symbol is composed of $K \leq N$ data symbols $a_{l,k}$ (l and k represent time index and subcarrier frequency index, respectively.). The output of the IFFT is discrete time with sampling time $T = T_u/N$. K is chosen small enough to provide the so-called "guard bands" at the edges of the transmission spectrum which is left free. Using these guard bands, the (periodic) spectrum is limited by using an appropriate analog transmission filter $G_T(\omega)$. The transmitted complex baseband signal can then be described by [32]

$$s(t) = \frac{1}{\sqrt{T_u}} \sum_{l=-\infty}^{\infty} \sum_{k=-K/2}^{K/2} a_{l,k} \Phi_{l,k}(t) * g_T(t) \tag{11}$$

where $*$ denotes convolution. Each data symbol is shaped by a rectangular pulse of length T_u and modulated onto a subcarrier with frequency $f_k = k/T_u$. In order to avoid intersymbol interference (ISI), the OFDM symbol is preceded by a guard interval of length T_g. Taking this into account, the resulting subcarrier pulses are

$$\Phi_{l,k}(t) = e^{j2\pi(k/T_u)(t-T_g-lT_s)} u(t - lT_s), \tag{12}$$

where

$$u(t) = \begin{cases} 1, & 0 \leq t < T_s \\ 0, & \text{else} \end{cases} \tag{13}$$

The resulting symbols are of length $T_s = T_u + T_g$, which is equivalent to $N_s = N + N_g$ samples.

Channel

To keep the model as simple as possible, we assume here that the signal is transmitted over a wide sense stationary uncorrelated scattering (WSS-US) Rayleigh fading channel with time varying impulse response $h(t, \tau)$ where:

1) The channel impulse response (CIR) is

$$h(t, \tau) = \sum_{n=0}^{L-1} h_n(t)\delta(\tau - nT_s), \tag{14}$$

where L is the number of distinct paths and $\{h_l(t), l = 0, 1, ..., L-1\}$ are mutually independent, WSS Gaussian complex random processes, having zero mean and statistical powers $\{\sigma_n^2 = \mathbb{E}\{|h_n(t)|^2\}, n = 0, 1, ..., L-1\}$.

2) The channel can be deemed static over each OFDM symbol interval (quasi static channel), so that during the transmission of the l-th OFDM symbol interval the CIR (14) can be approximated as

$$h(t, \tau) \cong h^{(l)}(\tau) = \sum_{n=0}^{L-1} h_n[l]\delta(\tau - nT_s) \tag{15}$$

where $h^{(l)}(\tau)$ and $h_n[l]$ denote the CIR and the value taken by the n-th tap gain $h_n(t)$ of (14), with $n = 0, 1, ..., L-1$, in the l-th OFDM symbol interval, respectively.

3) $N_g > L-1$, so that no inter-block interference is present in the detection of OFDM symbols.

Receiver

At the receive side, if the CFO does not exceed the subcarrier spacing and changes negligibly over each OFDM interval, it can be shown that the received signal, after down-conversion and low-pass filtering, can be expressed as [33]

$$r(t) = s(t - lT_s, \mathbf{a}_l, \mathbf{H}^l, \nu^l, \phi(t)) + \omega(t), \tag{16}$$

for $t \in [lT_s, (l+N)T_s]$, where

$$s(t, \mathbf{a}_l, \mathbf{H}^l, \nu^l, \phi(t)) = \frac{1}{\sqrt{NT_s}} e^{j\left(2\pi\nu^l t/NT_s + \phi(t)\right)} \sum_{k=0}^{N-1} a_{k,l} \mathrm{H}_k^l e^{j(2\pi f_k t)}. \tag{17}$$

In the above equation, $\mathbf{H}^l = [\mathrm{H}_1^l, \mathrm{H}_2^l, ..., \mathrm{H}_{N-1}^l]^T$ and H_n^l (with $n = 0, 1, ..., N-1$) is the channel frequency response at the n-th subcarrier frequency in the l-th symbol interval. In addition $\omega(t)$ is complex AWGN, and $\nu(t)$ and $\phi(l)$ are the phase noise process (due to both transmitter and receiver local oscillators) and the residual CFO (normalized to the OFDM symbol rate $1/NT_s$), respectively.

2.3.2 Carrier Frequency Offset (CFO)

CFO is mostly caused by the mismatch between the transmitter and the receiver mixer and, when not compensated, results in inter-carrier-interferences (ICI) and can seriously affect the transmission performance. There are several DA and

NDA methods presented in the literature for CFO estimation. In single-user OFDM systems, in the case of perfect estimation, the effect of CFO can be purely eliminated. On the other hand, in the multiple-user case, where each user introduces an independent CFO, it is not that easy and sometimes impossible for single receivers to mitigate the ICI. This is the case for orthogonal frequency division multiple access (OFDMA) uplink [34] (from independent users to base station). The same is true for OFDM in multi-relay cooperative network (where multiple relays propose independent CFOs for the receiver. In Chapter 5, the scenario of CFO-corrupted OFDM employing space-frequency coding over two relay channels is studied.

2.4 Conclusion

In this chapter, we have gone over some basic concepts related to the topics discussed in this thesis. In the subsequent chapters, we shall go in depth in these topics.

Chapter 3

Achievable Rates of MIMO Receivers with Linear Front-Ends

In this chapter, the rates achievable in MIMO systems with iterative receivers based on linear front-end (FE) processing is investigated. The iterative receiver in this setting involves two modules concatenated serially and cooperating iteratively. The inner module is merely a linear combiner based on MMSE detection or MRC. The outer module is assumed to be a SISO decoder. We investigate the achievable rates of this receiver when the transmitted signal is Gaussian distributed and there is a hypothetical erasure-type feedback from the decoder to the combiner. In this case, the achievable rate is approximated by the area below the EXIT curve of the linear FE receiver. We also consider a more practical case involving large-size QAM constellations where the information exchanged

between the receiver's modules is in the form of LLRs. In particular, we obtain theoretical approximate achievable rates for this scenario when the inner module employs either MMSE or MRC. We present several examples in which we verify the analytical results with simulations. We demonstrate that the iterative MIMO-MMSE receiver increases the achievable rate at medium SNRs as compared to the non-iterative receiver. We show, however, that both receivers achieve the same rates at low and high SNRs. As for the MIMO-MRC case, both iterative and non-iterative receivers perform about the same at low SNRs, whereas at high SNRs the rates saturate for both cases, with the iterative one being superior in all examples.

3.1 Introduction

Multiple-input multiple-output (MIMO) systems have been studied extensively over the last years. It has been shown both theoretically [4]- [2] and practically [8] that employing multiple transmit and receive antennas enables communicating with high information rates and/or improved reliability. This motivated the study of the capacity of MIMO systems [1], [2], [35]- [38].

In attaining the maximum achievable rate, specially while increasing the number of transmit antennas, practical problems appear through developing maximum likelihood sequence detection. The so-called turbo processing in the receiver

tries to ease this complex problem in a sub-optimal way where the detector and the decoder iteratively exchange information on the coded bits. The idea of such turbo MIMO receivers, e.g., [39], is an extension of the technique invented for decoding concatenated codes (e.g. "turbo" codes) [13] and used also for equalization [17], [40], synchronization [26], or multi user detection [41].

In fact, turbo processing may be theoretically equivalent to optimal sequence detection, that is, using the iterative receiver we might transmit with the maximum achievable rate. This may happen in two cases. In the first one, we would use the so-called horizontal encoding (that is using one encoder per antenna) and decode the transmitted sub-streams successively. As such, we would take advantage of the already detected sub-streams to remove the interference they cause to other sub-streams. Such successive interference cancellation (SIC) is capacity achieving as may be proved by applying the chain rule of mutual information. However, the requirement of using as many encoders as antennas is not appealing due to complexity issues. As an alternative, one may use a single channel encoder whose output is demultiplexed among all antennas, However, in this scenario, which is the focus of this thesis, one cannot apply SIC using decoded (thus reliable) bits estimates because all the sub-streams must be detected first before they are jointly decoded.

In such a case we still may transmit at the achievable rate provided the information exchanged about the bits/symbols is equivalent to the transmission over

the erasure channel and the devices of the turbo receiver operate in an optimal way (i.e., implement maximum likelihood detection) [22].[1] However, practically, the erasure-type information is not produced by the decoders/detectors and the reliability measures (the so called "soft" bits) are computed instead under the form of the logarithmic likelihood ratios (LLRs). This is in particular due to popularity of binary channel encoders and the soft-input soft-output (SISO) decoder. In addition, in the case in MIMO systems with many transmit antennas and high-order signal constellations, maximum likelihood implementation seems to be very complex. In such a case, sub-optimal, e.g. linear front-end detectors are an interesting alternative.

Despite many works on this subject, it is still not clear what the theoretically achievable transmission rates are if such a turbo-processing is applied, particularly when sub-optimal detectors are used. In this work we address this very issue. The idea of characterizing the achievable rate (or capacity) of sub-optimal receivers has appeared in the literature. Recently, the rates achievable in MIMO systems based on linear front-ends receiver were analyzed in [25], [42] for continuous Gaussian inputs. This paper extends these works into two directions. First, we integrate the concept of iterative processing for such receivers and evaluate the impact of their sub-optimality on the achievable rates. Next, exploiting the method of [43] to analytically evaluate the extrinsic information transfer (EXIT) function

[1] We may note that this is somewhat similar to the case of SIC as we deal then with the symbols we know perfectly or we do not know at all.

of the linear front-end, we apply it in the case of discrete constellations, which is a much more practical setup. We analyze the performance of such iterative systems and show that both iterative and non-iterative MIMO receivers based on minimum-mean square error (MMSE) perform the same in terms of the achievable rates at low and high signal-to-noise ratios (SNRs). It is also shown that for MIMO receivers based on maximal ratio combining (MRC), the achievable rate saturates for high SNRs for both iterative and non-iterative schemes and the former outperforms the latter for all range of SNR.

The rest of this chapter is organized as follows. In Section 3.2 we present the model of a MIMO system with linear front-ends and define its achievable rate. In Section 3.3, the iterative MIMO receivers with linear front-ends are introduced and the idea of EXIT analysis and the area property are explored. In Section 3.5, the achievable sum rate for more practical data models is analyzed. In Section 3.6 the achievable rates of iterative and non-iterative MIMO receivers based on MMSE and MRC principles are compared in various scenarios.

3.2 System Model

In the system we consider here, the information bits (or sequence) are first encoded by a rate-ρ channel encoder, interleaved, grouped into m-ary words, and then mapped into a complex point x drawn from constellation $\mathcal{X}$. The resulting

sequence of constellation points are then demultiplexed into N_t transmit antennas and sent through a linear channel with additive Gaussian noise. At the receiver, the i-th antenna captures the signal y_i, $i = 1, \ldots, N_r$ and the relationship between the involved signal is thus given by

$$\mathbf{y} = \mathbf{H}\mathbf{x} + \mathbf{n} = \sum_{k=1}^{N_t} \mathbf{h}_k x_k + \mathbf{n}, \tag{18}$$

where $\mathbf{y} = [y_1, y_2, ..., y_{N_r}]^T$, $\mathbf{H} = [\mathbf{h}_1, \mathbf{h}_2, ..., \mathbf{h}_{N_t}]$ is the $N_r \times N_t$ channel matrix, $\mathbf{x} = [x_1, x_2, ..., x_{N_t}]^T$ is the vector of transmitted symbols taken from constellation $\mathcal{X}$, and $\mathbf{n}$ is a vector of white Gaussian noise (AWGN), i.e., $\mathbb{E}\{\mathbf{n}\} = \mathbf{0}$ and $\text{Cov}\{\mathbf{n}\} = \mathbb{E}\{\mathbf{n}\mathbf{n}^\dagger\} = \text{N}_0\mathbf{I}$. The coded bits are assumed random and independent and the constellation $\mathcal{X}$ is normalized so that $\mathbf{x}$ may be treated as a random vector with $\text{Cov}\{\mathbf{x}\} = \sigma_x^2\mathbf{I} = \mathbf{I}$; Here, $(.)^T$ and $(.)^\dagger$ represent, respectively, the transpose and the transpose-conjugate of the vector/matrix. We assume perfect knowledge of $\mathbf{H}$ and N_0 at the receiver.

3.2.1 Linear Front-End and Achievable Rate

Using the linear front-ends we recover the transmitted symbols x_i via linear operations on $\mathbf{y}$. Knowing the second-order statistics of $\mathbf{x}$, the following operations will be performed [43]

$$\begin{aligned} \tilde{y}_i &= \mathbf{w}_i^\dagger \left[\mathbf{y} - \mathbf{H}_{[i]}\mathbb{E}\{\mathbf{x}_{[i]}\}\right] \\ &= \mathbf{w}_i^\dagger \mathbf{h}_i x_i + \sum_{\substack{k=1 \\ k\neq i}}^{N_t} \mathbf{w}_i^\dagger \mathbf{h}_k (x_k - \mathbb{E}\{x_k\}) + \mathbf{w}_i^\dagger \mathbf{n} \end{aligned} \tag{19}$$

where $(\cdot)_{[i]}$ denotes a vector (or a matrix) with the i-th element (or the i-th column) removed. The first, second, and third terms of the right hand side of (19) are, respectively, the desired signal, inter-symbol interferences, and the filtered noise. The knowledge of the mean of the symbols x_k for $k \neq i$ is possible thanks to the feedback from the channel decoder, otherwise, i.e., in non-iterative processing, we use $\mathbb{E}\{x_k\} = 0$.

Due to the processing in (19), the signal-to-interference-and-noise-ratio (SINR) for the i-th symbol is defined as

$$\gamma_i = \frac{|\mathbf{w}_i^\dagger \mathbf{h}_i|^2 \sigma_x^2}{\mathbf{w}_i^\dagger \mathbf{H}_{[i]} \mathrm{Cov}\{\mathbf{x}_{[i]}\} \mathbf{H}_{[i]}^\dagger \mathbf{w}_i + ||\mathbf{w}_i||^2 \mathrm{N}_0} \tag{20}$$

where $\mathrm{Cov}\{\mathbf{x}\}$ is the covariance of $\mathbf{x}$ and $||\cdot||^2$ is the Euclidean norm.

A priori knowledge about the symbols x_i in general diminish their variance, which, in turn, increases the post-processing SINR. In a non-iterative case, no a priori knowledge is available so $\mathrm{Cov}\{\mathbf{x}\} = \mathbf{I}$ but if iterative processing is applied, $\mathrm{Cov}\{\mathbf{x}\} = \kappa \mathbf{I}$ with $0 \leq \kappa \leq \sigma_x^2 = 1$.

Treating the interference as a Gaussian noise, the achievable rate of the linear receiver for a given $\mathbf{H}$ is given by

$$\mathrm{C}_{\mathbf{H}} = \sum_{i=1}^{N_t} \log_2(1 + \gamma_i), \tag{21}$$

and the ergodic channel capacity is given by

$$\mathrm{C} = \mathbb{E}\{\mathrm{C}_{\mathbf{H}}\} \tag{22}$$

where the expectation is taken with respect to $\mathbf{H}$.

While one may consider any type of linear processing, in the following, we consider two special cases, namely, MMSE and MRC since they are widely used.

MMSE receiver

While detecting the ith symbol and knowing the variance of the other symbols, the linear combiner may be obtained in the MMSE sense [44]

$$\begin{aligned}\mathbf{w}_i &= \arg\min_{\mathbf{w}} \mathbb{E}\left\{|\mathbf{w}^\dagger \mathbf{y} - x_i|^2\right\} \\ &= \left((\sigma_x^2 - \kappa)\mathbf{h}_i\mathbf{h}_i^\dagger + \kappa\mathbf{H}\mathbf{H}^\dagger + \mathrm{N}_0 I_{N_r}\right)^{-1}\mathbf{h}_i\sigma_x^2 \\ &= \frac{\sigma_x^2\mathbf{A}^{-1}\mathbf{h}_i}{1 + (\sigma_x^2 - \kappa)\mathbf{h}_i^\dagger\mathbf{A}^{-1}\mathbf{h}_i},\end{aligned} \tag{23}$$

where

$$\mathbf{A} = \kappa\mathbf{H}\mathbf{H}^\dagger + \mathrm{N}_0\mathbf{I}_{N_r}, \tag{24}$$

and the SINR for the ith sub-channel is

$$\gamma_i = \frac{\sigma_x^2\mathbf{h}_i^\dagger\mathbf{A}^{-1}\mathbf{h}_i}{1 - \kappa\mathbf{h}_i^\dagger\mathbf{A}^{-1}\mathbf{h}_i}. \tag{25}$$

In a non-iterative case $\kappa = \sigma_x^2$, so (25) reduces to [25]

$$\gamma_i = \frac{1}{\left[(I_{N_t} + \frac{\sigma_x^2}{\mathrm{N}_0}\mathbf{H}^\dagger\mathbf{H})^{-1}\right]_{i,i}} - 1, \tag{26}$$

where $[\mathbf{A}]_{i,i}$ denotes the ith diagonal element of $\mathbf{A}$.

A useful method for evaluating the ergodic capacity given by (22) in a closed-form for Gaussian input x is given in [25]. The idea developed in [25], hints

to a more general useful expression relating single-user capacity to multiple-user one. We develop this general relation in Chapter 4 and extend the result to simply proof the results appeared in [25] and derive the capacity of bit interleaved coded modulation (BICM) already shown in [49].

MRC receiver

The maximum ratio combining filter ignores the structure of the interference imposed by the form of the matrix $\mathbf{H}$ and sets $\mathbf{w}_i \equiv \mathbf{h}_i$. This is the simplest, although largely sub-optimal approach. The SINR for each sub-channel is then given by

$$\gamma_i = \frac{|\mathbf{h}_i|^4 \sigma_x^2}{|\mathbf{h}_i|^2 \mathrm{N}_0 + \mathbf{h}_i^\dagger \mathbf{H}_{[i]} \mathbf{H}_{[i]}^\dagger \mathbf{h}_i \kappa}. \tag{27}$$

Again for non-iterative receivers we set $\kappa = \sigma_x^2 = 1$.

3.3 Iterative Receivers

The model of an iterative MIMO receiver is shown in Figure 7 where the signal arriving at the receiver is fed to the linear combiner which exchanges information with the outer (channel) decoder in order to extract as much information as possible from the received signal. Such an iterative (turbo) processing should be, in general, characterized by the so-called density evolution (DE), that is, the probability density function (PDF) of the exchanged LLRs should be tracked

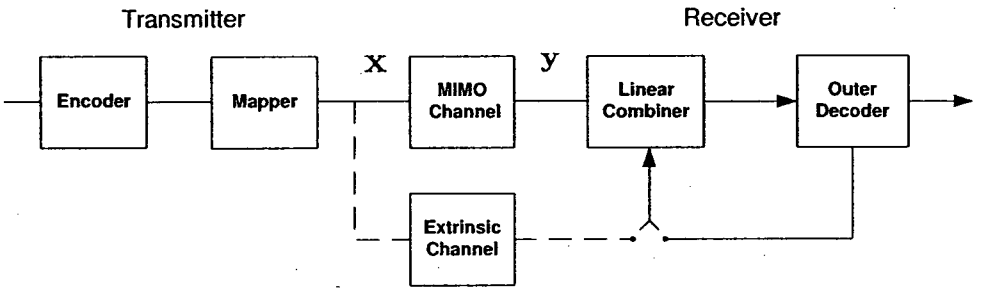

Figure 7: Model of MIMO transmission and schematic representation of the iterative receiver.

throughout the iterative process.

If the PDF of the LLRs may be parametrized, the DE is simplified, and if one parameter is sufficient, an appealing graphical representation of the iterative process is obtained. This is the spirit of the so-called EXIT charts that display information between the bits and their extrinsic LLRs produced by the devices participating in the iterative process. If the extrinsic LLRs had the form of the output of the erasure channel, EXIT charts would define exactly the density evolution and lend themselves to a useful interpretation: in particular, it is known that the area below the EXIT curves would correspond to the supported transmission rates of each device [22]. Generalization of these results to other cases was recently presented in [23]. This appealing property transforms the problem of the receiver design into the EXIT function (curves) fitting problem. This fundamental property is often used [24] even if, in practice, the extrinsic LLRs cannot be well modeled as outputs of the erasure channel (so the area property does not

hold exactly).

3.3.1 EXIT chart and the area property

To obtain the EXIT charts, for each block involved in the iterative process (here, the linear combiner and the outer decoder) the extrinsic information obtained from the other block is artificially generated as if it was obtained from the so-called extrinsic channel [22], cf. Fig. 7.

Let us assume that the extrinsic channel is of an erasure-type, i.e., where the symbol appears at the output correctly with probability $1-p$ and it is erased with probability p. The EXIT function for arbitrary input signal $\mathbf{x}$ is given by

$$I_{\text{out}} = \mathrm{T}(I_{\text{in}}) = \sum_{i=1}^{N_t} I(x_i; \mathbf{y}|\mathbf{x}_{[i]}^{\text{Er}}), \tag{28}$$

where $I(x_i; \mathbf{y}|\mathbf{x}_{[i]}^{\text{Er}})$ is the mutual information conditioned on the output of the extrinsic channel $\mathbf{x}_{[i]}^{\text{Er}}$ and the erasure (with probability p) applies to x_k for any $k \neq i$. Then, since $I_{\text{in}} = 1-p$, the area theorem [23] states that

$$\mathrm{C} = I(\mathbf{x}; \mathbf{y}) = \int_0^1 \mathrm{T}(I_{\text{in}})\mathrm{d}p. \tag{29}$$

It is easy to show that for MMSE receivers, when $\mathbf{x}$ is zero mean Gaussian with covariance matrix $\sigma_x^2\mathbf{I}$, the output of the MMSE filter for ith sub-channel, $\tilde{y}_i$ is the sufficient statistic of symbol x_i, $\forall i \in \{1, 2, ..., n\}$. In other words, in this case, all the information about the transmitted symbol x_i, extractable from the

output vector $\mathbf{y}$, can be extracted from the filtered symbol $\tilde{y}_i$. That is,

$$I(x_i; \mathbf{y}|\mathbf{x}_{[i]}^{\mathrm{Er}}) = I(x_i; \tilde{y}_i|\mathbf{x}_{[i]}^{\mathrm{Er}}). \tag{30}$$

This means that for Gaussian input $\mathbf{x}$, the optimum (maximum likelihood) and MMSE receivers have the same performance. In this situation the EXIT function of (28) reduces to

$$I_{\mathrm{out}} = \sum_{i=1}^{N_t} I(x_i; \tilde{y}_i|\mathbf{x}_{[i]}^{\mathrm{Er}}). \tag{31}$$

Thus, assuming that the extrinsic information is of the erasure-type, and assuming that the optimum outer decoder's EXIT curve fits the MMSE's EXIT function, from (29) we know that the iterative MMSE receiver for Gaussian input would reach the optimum MIMO channel capacity known as

$$\mathrm{C}_{\mathbf{H}} = \log_2(\det(\mathbf{I} + \sigma_x^2 \frac{\mathbf{H}^{\dagger}\mathbf{H}}{\mathrm{N}_0})). \tag{32}$$

3.3.2 EXIT functions of sub-optimal MMSE receiver

Up to now, we repeated the results known in the case of the erasure-type extrinsic information. Since, in practice, the information about the bits/symbols has a different form, we will make another step towards the analysis of the more realistic scenarios. Note that in (28) and (31), the receiver performs the MMSE filtering for *each* combination of erased and non-erased symbols in $\mathbf{x}_{[i]}^{\mathrm{Er}}$. Thus, there is not much reduction in the computational effort at the front-end (which is the fundamental motivation behind the use of MMSE receivers). Yielding for such the

simplification of the receiver, we assume that the linear combiners $\mathbf{w}_i$ are designed knowing only the probability of erasure and not which symbol was erased. To deal with this information in the MMSE sense, we proceed as shown in (19) but we use the average variances of the symbols

$$\begin{aligned}\kappa &= \mathbb{E}\left\{|x_i - \mathbb{E}\{x_i\}|^2\right\} = (1-p)0 + p\mathbb{E}\left\{|x_i|^2\right\} \\ &= p\sigma_x^2. \end{aligned} \tag{33}$$

The EXIT function of the MMSE receiver for this case would be

$$I_{\text{out}} = \sum_{i=1}^{N_t} I(x_i; \mathbf{y}|p) = \sum_{i=1}^{N_t} I(x_i; \tilde{y}_i|p), \tag{34}$$

where, with a slight abuse of notation, we use $I(\cdot;\cdot|p)$ to indicate that the mutual information is calculated without conditioning on the random variables but depends only on the parameter p. Further, we may write

$$I_{\text{out}} = \sum_{i=1}^{N_t} \log_2(1+\gamma_i), \tag{35}$$

where γ_i is the SINR for the ith sub-channel.

From the data processing theorem, the EXIT function calculated this way (i.e., using solely p) will be smaller than the one conditioned on $\mathbf{x}_{[i]}^{\text{Er}}$ because the receiver does not use the entire information provided by the erasure channel and only computes the first and the second statistics of the extrinsic channel's output.

Thus, the rate achievable by the iterative MIMO MMSE would be

$$\begin{aligned} \mathrm{C}'_{\mathbf{H}} &= \int_0^1 \sum_{i=1}^{N_t} I(x_i; \mathbf{y}|p)\mathrm{d}p \\ &= \frac{1}{\sigma_x^2} \int_0^1 \sum_{i=1}^{N_t} I(x_i; \mathbf{y}|p)\mathrm{d}\kappa, \end{aligned} \tag{36}$$

must satisfy $\mathrm{C}'_{\mathbf{H}} < \mathrm{C}_{\mathbf{H}}$.

Further, the ergodic achievable rate C′ is calculated by averaging over realizations of **H**. We compare C and C′ in Sec. 3.6.

It is interesting to note that we do not need to resort to Monte-Carlo simulations to obtain C′ as we can express the integrand of (36) in a compact form as shown in next section. Note that the value of the EXIT functions for $p = 1$ (or equivalently $\kappa = \sigma_x^2$) indicate the achievable rate when there is no information available from the outer decoder, which is the performance of the non-iterative receiver.

3.4 Efficient Calculation of the Achievable Rate in MMSE Receiver

Assuming $\sigma_x^2 = 1$ and applying the chain rule of mutual information to (36) we obtain

$$\mathrm{C}'_{\mathbf{H}} = \int_0^1 \sum_{i=1}^{N_t} \left[I(\mathbf{x}; \mathbf{y}|p) - I(\mathbf{x}_{[i]}; \mathbf{y}|x_i, p) \right] \mathrm{d}\kappa, \tag{37}$$

or

$$C'_{\mathbf{H}} = \int_0^1 \sum_{i=1}^{N_t} \Big[I(\mathbf{x};\mathbf{y}|\mathrm{Cov}\{\mathbf{x}\} = \hat{\mathbf{I}}_{N_t,i}) - I(\mathbf{x}_{[i]};\mathbf{y}|\mathrm{Cov}\{\mathbf{x}_{[i]}\} = \kappa \mathbf{I}_{N_t-1}) \Big] \, \mathrm{d}\kappa, \quad (38)$$

where $\mathrm{Cov}\{\mathbf{x}\}$ is the covariance of $\mathbf{x}$ and

$$\hat{\mathbf{I}}_{N_t,i} = \mathrm{diag}([\kappa, \ldots, \kappa, \underbrace{\sigma_x^2 = 1}_{ith}, \kappa, \ldots, \kappa]). \quad (39)$$

Then, (38) can be reduced to

$$C'_{\mathbf{H}} = \int_0^1 \sum_{i=1}^{N_t} \left[\log_2 \left(\det(\mathrm{I}_{N_t} + \frac{\mathbf{H}\hat{\mathrm{I}}_{N_t,i}\mathbf{H}^\dagger}{\mathrm{N}_0}) \right) - \log_2 \left(\det(\mathrm{I}_{N_t} + \kappa \frac{\mathbf{H}_{[i]}\mathbf{H}_{[i]}^\dagger}{\mathrm{N}_0}) \right) \right] \mathrm{d}\kappa. \quad (40)$$

We are interested in computing the Ergodic channel capacity of (22). Let us assume an uncorrelated Rayleigh fading MIMO channel as follows.

$$\mathbf{H} \sim \mathcal{CN}(0, I_{N_\mathrm{r}} \otimes I_{N_t}), \quad (41)$$

where $\otimes$ represents Kronecker product. $\mathbf{H}$ is normalized to satisfy $\mathbb{E}\left\{\mathrm{tr}(\mathbf{H}\mathbf{H}^\dagger)\right\} = N_\mathrm{r}N_\mathrm{t}$. Armed with this result, we can write (40) as

$$\begin{aligned} C' = N_\mathrm{t} \int_0^1 \mathbb{E} \left[\log_2 \left(\det(\mathrm{I}_{N_t} + \frac{\mathbf{H}\hat{\mathrm{I}}_{N_t,1}\mathbf{H}^\dagger}{\mathrm{N}_0}) \right) \right] \mathrm{d}\kappa \\ - N_\mathrm{t} \int_0^1 \mathbb{E} \left[\log_2 \left(\det(\mathrm{I}_{N_t} + \kappa \frac{\mathbf{H}_{[1]}\mathbf{H}_{[1]}^\dagger}{\mathrm{N}_0}) \right) \right] \mathrm{d}\kappa. \end{aligned} \quad (42)$$

Figure 8 shows the achievable rates for an $N \times N$ uncorrelated Rayleigh fading MIMO channel which is the result of (42) where the expectation is replaced by averaging. To simplify (42), let us denote $\tilde{\mathbf{H}}_i = \hat{\mathrm{I}}_{N_t,i}^{1/2}\mathbf{H}$, where $(.)^{1/2}$ represents the square root of the matrix. Consequently,

$$\tilde{\mathbf{H}}_1 \sim \mathcal{CN}(0, \hat{\mathrm{I}}_{N_t,1} \otimes \mathrm{I}_{N_t}), \quad (43)$$

which can be viewed as correlated Rayleigh fading channel with transmit correlation matrix $\hat{\mathrm{I}}_{N_t,1}$. This suggests that the first term in (42) is simply the ergodic channel capacity of a MIMO system with N_t transmit and N_r receive antennas in correlated Rayleigh fading channel with covariance matrix $\hat{\mathrm{I}}_{N_t,1}$ at the transmit side, which was studied in detail in [45] and [36].

Note that the diagonal matrix $\hat{\mathrm{I}}_{N_t,1}$ in (39), has $N_t - 1$ eigenvalues κ, and one $\sigma_x^2 = 1$. As it is mentioned in [36], evaluating the characteristic function of such a random variable (the first term of C'_{H}) would need the limiting case when the eigenvalues tends to be equal. From numerical computation point of view, it only needs a small disturbing in the values of the equal eigenvalues and changing them to very close distinct numbers.

As for the second term in (42), it is essentially the ergodic channel capacity of a MIMO system with $N_t - 1$ transmit and N_r receive antennas in uncorrelated Rayleigh fading channel, which is also studied in the literature in detail in [1], [36] and [25].

We note that both terms in (42) has closed-form mathematical representation in the literature. We can also mention that the method introduced in the [25] can be derived by applying the above method for the values of (42) computed in the point $\kappa = \sigma_x^2$ instead of integration of the equation (42) (the point of the EXIT where we have no extrinsic information, which represents the performance of non-iterative receiver).

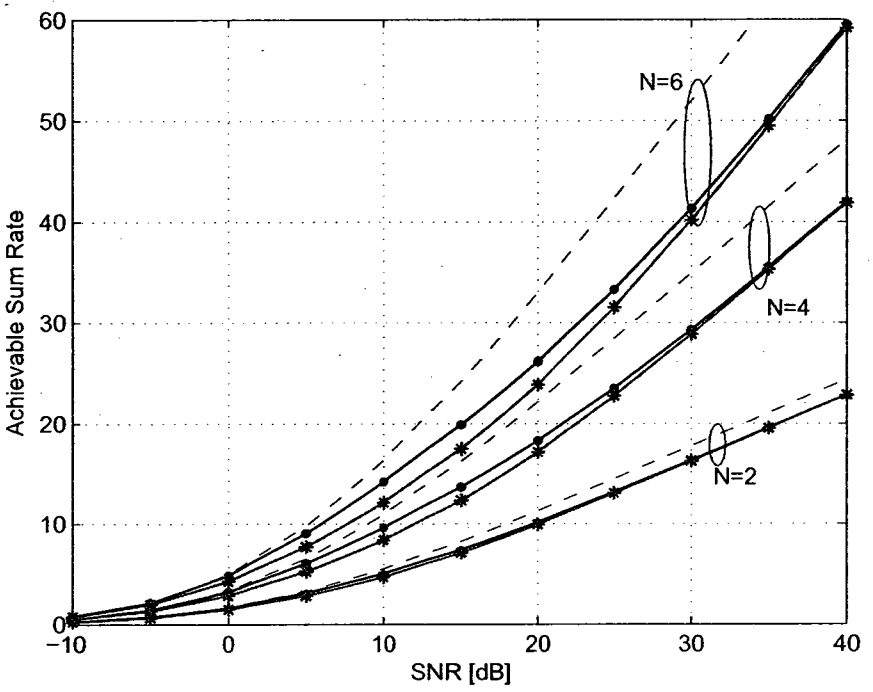

Figure 8: Achievable sum rate for a Gaussian input $N \times N$ uncorrelated Rayleigh fading MIMO channel for, a) non-iterative MMSE receiver (solid line with stars), b) iterative MMSE receivers (solid line with circles) and c) MIMO channel Shannon capacity (dashed line).

3.5 Iterative MIMO Receiver in BICM transmission

Although assuming that constellation $\mathcal{X}$ has Gaussian distribution and that the extrinsic channel is of erasure-type gives an insight into the achievable rates, we want to consider a much more practical setup. Thus, we drop two simplifying assumptions used before. First of all, we consider quadrature-amplitude modulation (QAM) $\mathcal{X}$ with uniformly distributed constellation points which is definitely a practical case to be considered. Secondly, we assume that the extrinsic channel provides information for the bits and the corresponding LLRs have Gaussian distribution characterized by a single parameter σ_{I}^2 [20], [21], that is,

$$\mathrm{p}(\lambda|1) = \phi(\lambda) = \frac{1}{\sqrt{2\pi\sigma_{\mathrm{I}}^2}} \exp(-\frac{|\lambda - 0.5\sigma_{\mathrm{I}}^2|^2}{2\sigma_{\mathrm{I}}^2}). \tag{44}$$

Then, the mutual information between the extrinsic LLRs and the coded bits is given by

$$\begin{aligned} I_{\mathrm{in}} = I(\lambda^{\mathrm{ext}}; c) &= 1 - \mathbb{E}\left\{\log_2(1 + e^{-\lambda})\right\} \\ &= \mathbb{E}\left\{\log_2(1 + \tanh(\lambda/2))\right\}, \end{aligned} \tag{45}$$

where the expectation is taken with respect to the extrinsic LLRs.

To evaluate the EXIT function I_{out} of the FE detector (that comprises the linear combiner and the demapper which calculates the extrinsic LLRs from the MMSE output $\tilde{y}_i$ considering the interfering symbols as a Gaussian noise), we

proceed in the following steps:

$$\kappa = \mathrm{V}(I_{\mathrm{in}}) \tag{46}$$

$$I_{\mathrm{out}} = \mathrm{G}(\kappa) = \sum_{i=1}^{N_t} \log_2(1 + \gamma_i \cdot \epsilon(\gamma_i)), \tag{47}$$

where $\mathrm{V}(\cdot)$ represents the symbols' variance κ that, for a given constellation, depends completely on I_{in} (through the parameter σ_{I}^2), and $\mathrm{G}(\cdot)$ relates the variance of the symbols κ to the output mutual information for one specific channel realization $\mathbf{H}$ and value of N_0. The SNR gap $\epsilon(\gamma)$ due to the constellation being non-Gaussian (the so-called constellation-constrained capacity (CM)) is a function of SNR and takes values between 1 (for low SNRs) and $\epsilon_\infty = (\frac{\pi e}{6})^{-1} = 0.7026 = -1.5329\mathrm{dB}$ for SNRs approaching infinity (cf., Fig. 9) [46].

For any 2^m-dimensional constellation $\mathcal{X} = \{\alpha_1, \ldots, \alpha_{2^m}\}$ and bit mapping $\mu : [b_{n,1}, \ldots, b_{n,m}] \rightarrow \alpha_n$, the function $\mathrm{V}(\cdot)$ can be characterized as follows [43]

$$\kappa = 1 - \sum_{n=1}^{2^m} \sum_{k=1}^{2^m} \alpha_n \alpha_k^* \prod_{l=1}^{N} \Phi(b_{k,l} \oplus b_{n,l}; \sigma_{\mathrm{I}}^2) \tag{48}$$

where $b_{n,l}$ is the l-th bit of the binary label of α_n, $\oplus$ represents binary exclusive-or, and

$$\Phi(b; \sigma_{\mathrm{I}}^2) = \frac{1}{2} \int_{-\infty}^{\infty} \frac{e^{\lambda b} + e^{\lambda(2-b)}}{(1+e^{\lambda})^2} \phi(\lambda) d\lambda. \tag{49}$$

Note that bit-interleaved coded modulation (BICM) is a practical choice (in particular when Gray labeling is applied) but it does not allow us to reach the

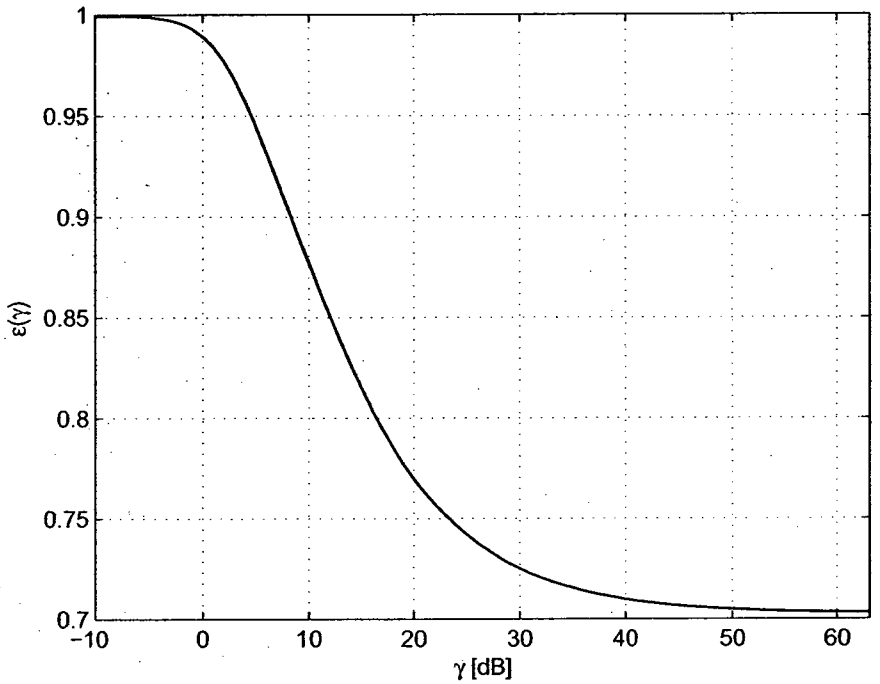

Figure 9: SNR gap $\epsilon(\gamma)$ between Gaussian and CM capacities.

CM capacity. In fact, while for a given SNR, the CM capacity increases with the constellation size, BICM capacity does not and there is an optimal constellation size that maximizes the BICM capacity [47]. On the other hand, using again the area property we may conjecture that BICM with iterative decoding/demapping (BICM-ID) bridges the gap from BICM to CM [24]. Therefore, we can safely use the gap $\epsilon(\gamma)$ for calculating the achievable rate in BICM transmission.

The achievable rate for these receivers can be next approximated by the area under the EXIT function

$$\mathrm{C_H} = \sum_{i=1}^{N_t} \int_0^1 \log_2(1 + \epsilon(\gamma_i) \cdot \gamma_i) \mathrm{d}I_{\mathrm{in}}, \tag{50}$$

where γ_i (the SINR for the ith sub-channel) should be replaced by (25) and (27) for MMSE and MRC receivers, respectively. The ergodic channel capacity is calculated using (22).

Figure 10 shows the EXIT functions we obtained numerically for one specific channel realization and different values of $\mathrm{N_0}$. Of course, the rate achievable using non-iterative receiver is represented by the EXIT function for $I_{\mathrm{in}} = 0$ (i.e., when the combiner does not have any extrinsic information available).

In the following we show that, the somewhat cumbersome relationships $I_{\mathrm{in}} \to \sigma_{\mathrm{I}}^2$ in (45), and $\sigma_{\mathrm{I}}^2 \to \kappa$ in (48) may be simplified thanks to Observation 1 given below. Also, the conclusions about asymptotic (in SNR) behavior of MMSE receiver may be drawn, cf., Observation 2.

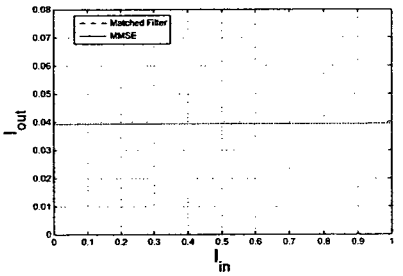

(a)

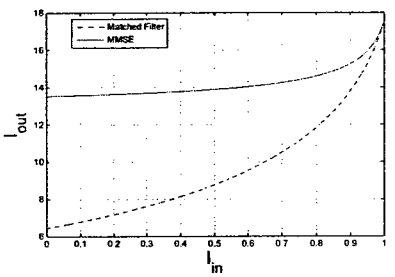

(b)

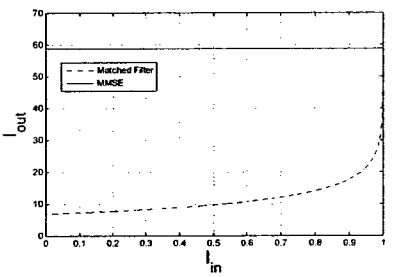

(c)

Figure 10: EXIT charts for MMSE and MRC and for SNRs a)−20dB, b)15dB and c)50dB.

Observation 1 *For large-size uniform QAM constellation with Gray labeling, κ is well approximated by a linear function of I_{in} as*

$$\kappa \approx 1 - I_{in}. \tag{51}$$

Proof. Assume we have 4^m-size Gray-labeled QAM constellation $\mathcal{X} = \mathcal{A} \times \mathcal{A}$, which, for $m > 1$ may be obtained from size 4^{m-1} constellation by placing it in first quarter of complex plane and turning over each axis in order to have 4^m constellation points. Considering the first two bits of each 4^m points to be $\{00, 01, 11, 10\}$ for first, second, third and fourth quarter of the plane respectively (cf., Fig. 11). Let $2m$ be the number of bit representing constellation $x \in \mathcal{X}$, where $L = 2^{m-1}$ and $\mathcal{A} = \{-(2L-1)a, ..., -3a, -a, a, 3a, ..., (2L-1)a\}$.

Applying uniform power constraint we will have:

$$a^2 = \frac{1}{2(\frac{4}{3}(2^{m-1}+1)(2^{m-1}-1)+1)}. \tag{52}$$

For the mentioned Gray-labeled constellation (48) reduces to

$$1 - \kappa_m = \sum_{n=1}^{4^m}\sum_{k=1}^{4^m} \alpha_n \alpha_k^* \prod_{l=1}^{2m} \Phi(b_{k,l} \oplus b_{n,l}; \sigma_{\mathrm{I}}^2) \tag{53}$$

$$= 4((\Phi(0;\sigma_{\mathrm{I}}^2))^2 - (\Phi(1;\sigma_{\mathrm{I}}^2))^2) \sum_{n=1}^{4^{m-1}}\sum_{k=1}^{4^{m-1}} \tilde{\alpha}_n \tilde{\alpha}_k^* \prod_{l=1}^{2(m-1)} \Phi(b_{k,l} \oplus b_{n,l}; \sigma_{\mathrm{I}}^2) \tag{54}$$

$$= 2\beta \sum_{n=1}^{4^{m-1}}\sum_{k=1}^{4^{m-1}} \tilde{\alpha}_n \tilde{\alpha}_k^* \prod_{l=1}^{2(m-1)} \Phi(b_{k,l} \oplus b_{n,l}; \sigma_{\mathrm{I}}^2), \tag{55}$$

where

$$\beta = \Phi(0;\sigma_{\mathrm{I}}^2) - \Phi(1;\sigma_{\mathrm{I}}^2) = \frac{1}{2}\int_{\infty}^{\infty} (\frac{1-e^{\lambda}}{1+e^{\lambda}})^2 \phi(\lambda|1)\mathrm{d}\lambda = \frac{1}{2}\mathbb{E}\left\{(\frac{1-e^{\lambda}}{1+e^{\lambda}})^2\right\}. \tag{56}$$

Defining $X = L \cdot a \cdot (1 + \imath)$, in the equations $\tilde{\alpha}$ belongs to a 4^{m-1}-size Gray-labeled constellation whose origin is in $X_1 = \frac{1}{2}X$, we have:

$$|\mathbb{E}\{\tilde{\alpha}\}|^2 = |\mathbb{E}\{X_1 + \alpha\}|^2 = |X_1|^2 + |\mathbb{E}\{\alpha\}|^2. \tag{57}$$

So we will have

$$\begin{aligned} 1 - \kappa_m &= 2\beta \left[\frac{|X|^2}{4} + \sum_{n=1}^{4^{m-1}} \sum_{k=1}^{4^{m-1}} \alpha_n \alpha_k^* \prod_{l=1}^{2(m-1)} \Phi(b_{k,l} \oplus b_{n,l}; \sigma_1^2) \right] \\ &= 2\beta \left[\frac{|X|^2}{4} + 2\beta \sum_{n=1}^{4^{m-2}} \sum_{k=1}^{4^{m-2}} \tilde{\alpha}_n \tilde{\alpha}_k^* \prod_{l=1}^{2(m-2)} \Phi(b_{k,l} \oplus b_{n,l}; \sigma_1^2) \right] \\ &= 2\beta \left[\frac{|X|^2}{4} + 2\beta \left[\frac{|X|^2}{4^2} \sum_{n=1}^{4^{m-2}} \sum_{k=1}^{4^{m-2}} \alpha_n \alpha_k^* \prod_{l=1}^{2(m-2)} \Phi(b_{k,l} \oplus b_{n,l}; \sigma_1^2) \right] \right]. \end{aligned} \tag{58}$$

Recursively reducing the constellation size involved, we obtain the sum of geometric series that yield

$$\begin{aligned} 1 - \kappa_m &= |X|^2 \sum_{k=1}^{m} (\frac{\gamma}{2})^k \\ &= |X|^2 \frac{\frac{\gamma}{2}(1 - (\frac{\gamma}{2})^m)}{1 - \frac{\gamma}{2}} \\ &= \frac{2^{2m} \frac{\gamma}{2}(1 - (\frac{\gamma}{2})^m)}{(1 - \frac{\gamma}{2})(\frac{4}{3}(2^{m-1} + 1)(2^{m-1} - 1) + 1)}, \end{aligned} \tag{59}$$

Figure 12 shows the difference between κ_m and $1 - I_{\text{in}}$ as a function of I_{in}. As constellation size grows we have

$$\lim_{m \to \infty} (1 - \kappa_m) = \frac{\frac{3\beta}{2}}{(1 - \frac{\beta}{2})}. \tag{60}$$

It may be appreciated that for large m, the relative error of linear approximation (27) is smaller than 1%, which is an acceptable inaccuracy within the set of

approximations adopted for the analysis. Figure 13 shows the ratio of κ_m over $1 - I_{\text{in}}$ as a function of I_{in}. Linear assumtion is simply consideing the following approximation

$$\frac{3E_\phi\left\{(\frac{1-e^\lambda}{1+e^\lambda})^2\right\}}{4-E_\phi\left\{(\frac{1-e^\lambda}{1+e^\lambda})^2\right\}} \approx 1 - E_\phi\left\{\log_2(1+e^{-\lambda})\right\}, \tag{61}$$

which is sown in Figure 14.

Applying this approximation reduces (50) to

$$\mathrm{C_H} \approx \sum_{i=1}^{N_t} \int_0^1 \log_2(1+\epsilon(\gamma_i)\cdot\gamma_i)\mathrm{d}\kappa. \tag{62}$$

Observation 2 *In low and high SNR, the rates achievable by iterative and non-iterative MIMO receivers are the same.*

Proof. First assume high SNR regime where $\mathrm{N_0} \to 0$. In this case $\gamma_i \to \infty, \forall i \in \{1, 2, ..., N_t\}$ as the denominator of (25) goes to zero and then $\epsilon(\gamma_i) = \epsilon_\infty, \forall i$. The achievable sum rate of equation (62) for each channel realization reduces to

$$\begin{aligned}
\mathrm{C_H} &= \sum_{i=1}^{N_t} \int_0^1 \log_2(1+\epsilon_\infty\gamma_i)\mathrm{d}\kappa \\
&= \sum_{i=1}^{N_t} \int_0^1 \log_2(\frac{1+(\epsilon_\infty-\kappa)\mathbf{h}_i^\dagger\mathbf{A}^{-1}\mathbf{h}_i}{1-\kappa\mathbf{h}_i^\dagger\mathbf{A}^{-1}\mathbf{h}_i})\mathrm{d}\kappa \\
&= \int_0^1 \log_2(\prod_i \frac{1+(\epsilon_\infty-\kappa)\mathbf{h}_i^\dagger\mathbf{A}^{-1}\mathbf{h}_i}{1-\kappa\mathbf{h}_i^\dagger\mathbf{A}^{-1}\mathbf{h}_i})\mathrm{d}\kappa \\
&= \int_0^1 \log_2 \frac{\det\left(\mathrm{diag}((\mathrm{I}+\frac{\mathbf{H}^\dagger\mathbf{H}}{\mathrm{N_0}}\epsilon_\infty)(\mathrm{I}+\frac{\mathbf{H}^\dagger\mathbf{H}}{\mathrm{N_0}}\kappa)^{-1})\right)}{\det\left(\mathrm{diag}(\mathrm{I}+\frac{\mathbf{H}^\dagger\mathbf{H}}{\mathrm{N_0}}\kappa)^{-1}\right)}\mathrm{d}\kappa.
\end{aligned} \tag{63}$$

We can then see that for each small positive number $\kappa_{\min}$, exists a small value for $\mathrm{N_0}$ (or equivalently a very large SNR $= \frac{1}{\mathrm{N_0}}$), such that the elements of the matrix

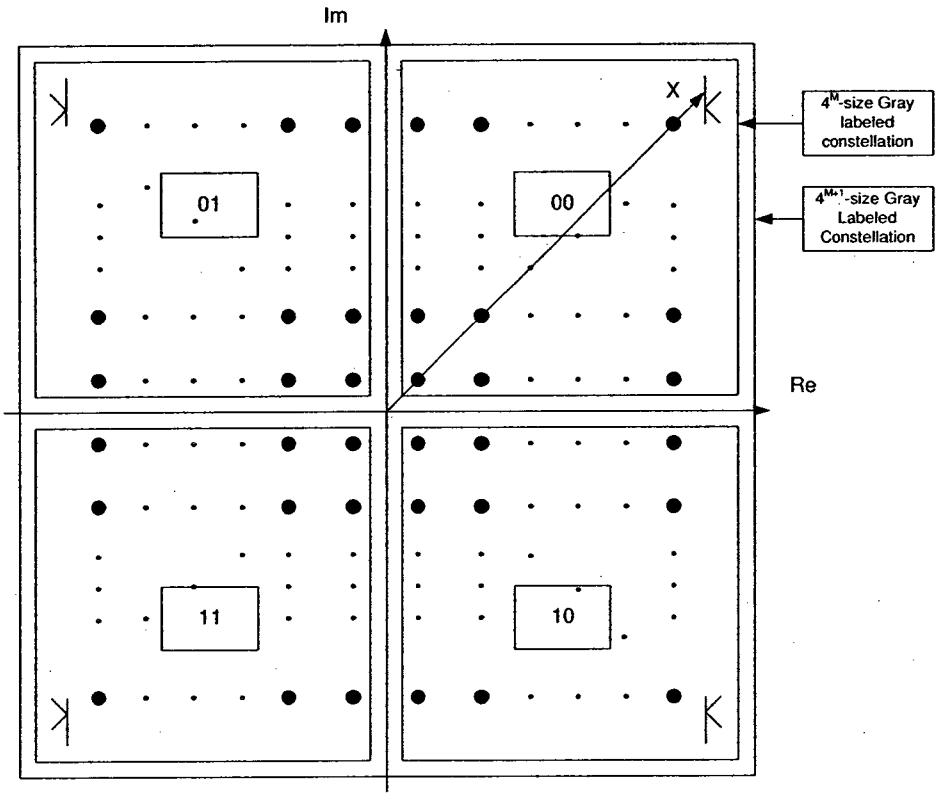

Figure 11: Generating 4^{m+1}-size Gray-labeled uniform (QAM) constellation from 4^m-size one. The letter k appearing in the first quarter shows how each plane is turned over. Digits in the boxes represents the first and second bits added to the new constellation points. The vector X is shown in the figure.

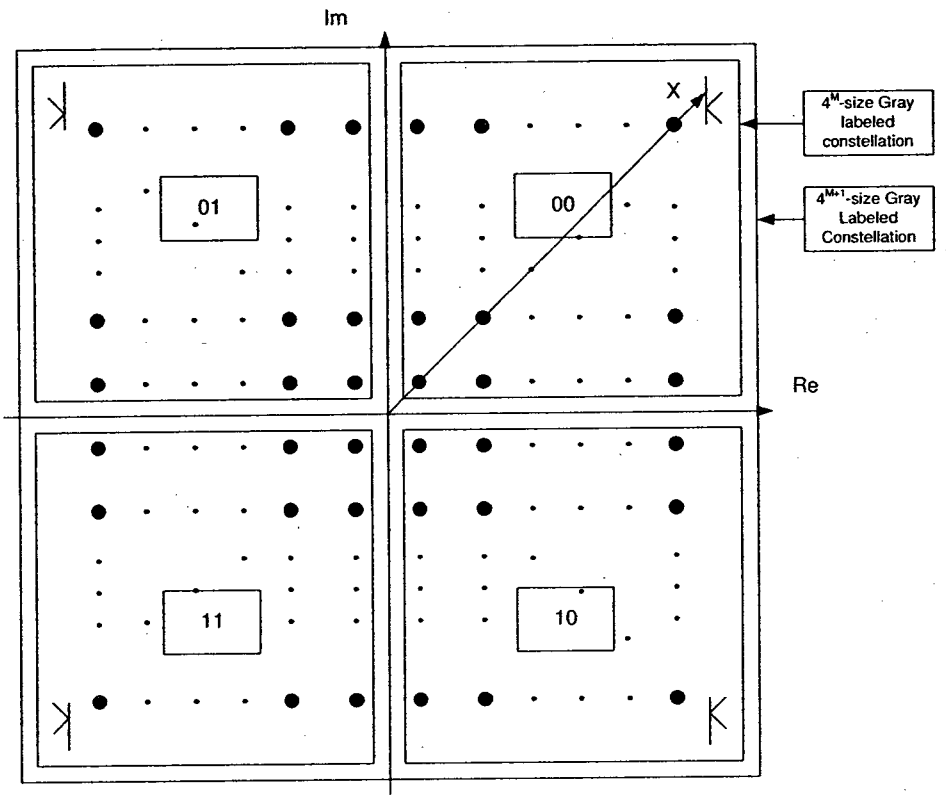

Figure 11: Generating 4^{m+1}-size Gray-labeled uniform (QAM) constellation from 4^m-size one. The letter k appearing in the first quarter shows how each plane is turned over. Digits in the boxes represents the first and second bits added to the new constellation points. The vector X is shown in the figure.

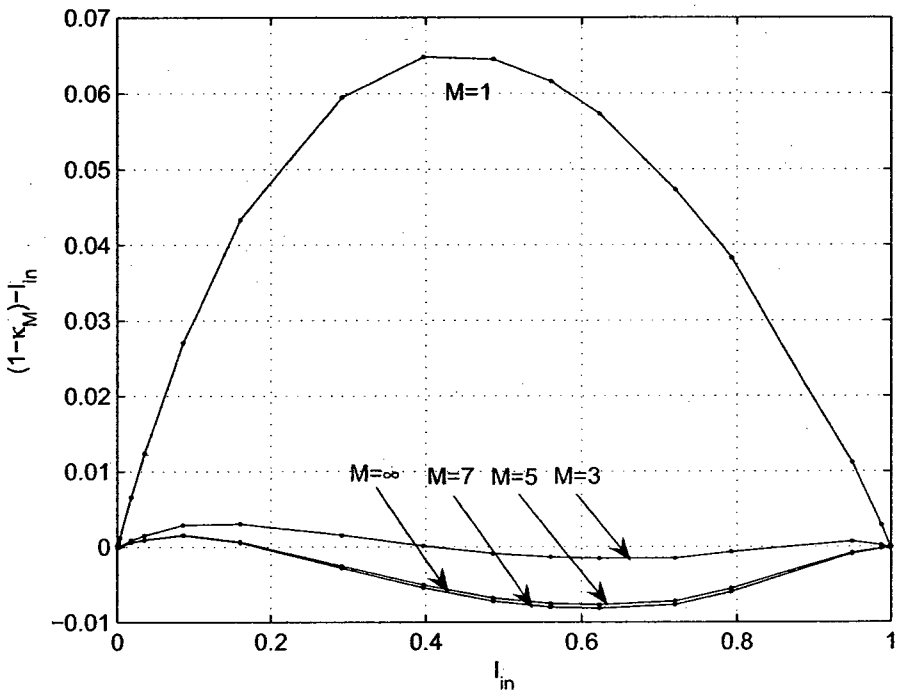

Figure 12: The difference of $1-\kappa$ and I_{in} as a function of I_{in} for different Ms.

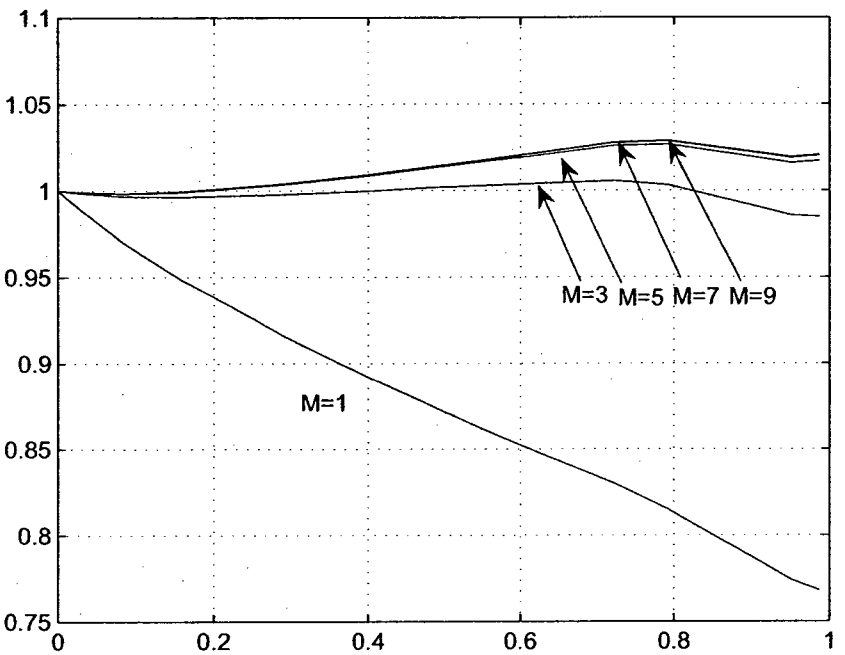

Figure 13: The ratio of $1-\kappa$ and I_{in} as a function of I_{in} for different Ms..

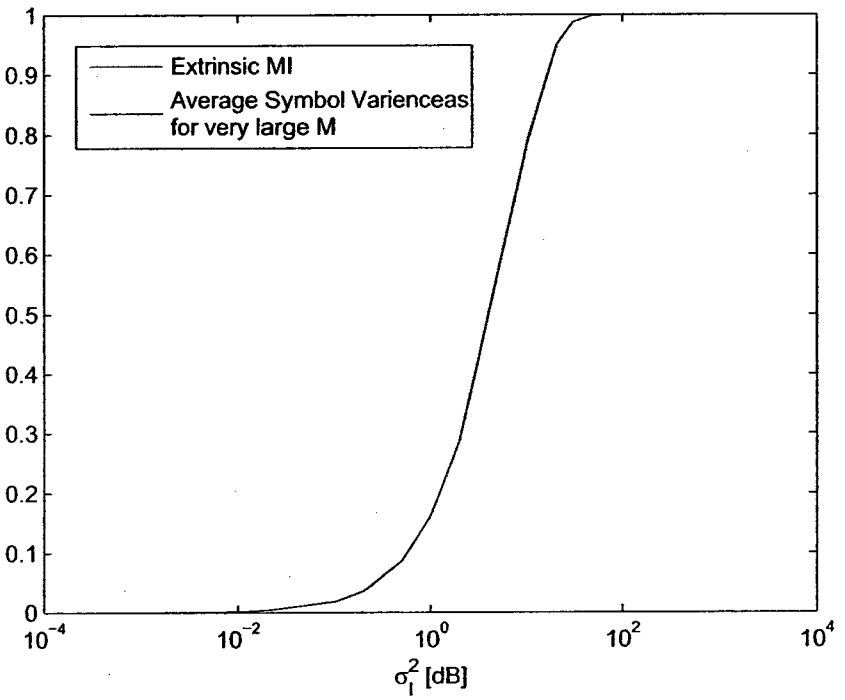

Figure 14: Two sides of (61) as a function of σ_I^2.

$\frac{\mathbf{H}^\dagger\mathbf{H}}{\mathrm{N}_0}\kappa$ are much greater than I_{N_t} so we can approximate (63) as

$$\begin{aligned}
\mathrm{C}_\mathbf{H} &\approx \int_{\kappa_{\min}}^{1} \log_2 \frac{\det\left(\mathrm{diag}((\frac{\mathbf{H}^\dagger\mathbf{H}}{\mathrm{N}_0}\epsilon_\infty)(\frac{\mathbf{H}^\dagger\mathbf{H}}{\mathrm{N}_0}\kappa)^{-1})\right)}{\det\left(\mathrm{diag}(\frac{\mathbf{H}^\dagger\mathbf{H}}{\mathrm{N}_0}\kappa)^{-1}\right)} \mathrm{d}\kappa \\
&= (1-\kappa_{\min})\log_2 \frac{\det\left(\mathrm{diag}(\epsilon_\infty \mathbf{I}_{N_t})\right)}{\det\left(\mathrm{diag}((\frac{\mathbf{H}^\dagger\mathbf{H}}{\mathrm{N}_0})^{-1})\right)} \\
&\approx N_t \log_2 \epsilon_\infty - \log_2\left(\det(\mathrm{diag}(\frac{\mathbf{H}^\dagger\mathbf{H}}{\mathrm{N}_0})^{-1})\right), \qquad (64)
\end{aligned}$$

where the approximation in (64) holds when $N_0 \to 0$ since then $\kappa_{\min} \to 0$.

From (64) we conclude that for high SNRs the iterative receiver performs the same as the non-iterative ones. Actually, this is not surprising because we know that the MMSE receiver for the high SNR regime ignores the noise and eliminates the interferences which, having no impact on the output, does not need to be mitigated by the iterative receiver.

Assume now that SNR is low, i.e., $\mathrm{N}_0 \to \infty$. Then, $\gamma_m \to 0, \forall m \in \{1, 2, \ldots, N_t\}$ as the numerator of (25) goes to zero and then $\epsilon(0) = 1$. In this case we can simplify (62) as

$$\mathrm{C}_\mathbf{H} \approx \int_0^1 \log_2 \frac{\det\left(\mathrm{diag}((\mathbf{I}+\frac{\mathbf{H}^\dagger\mathbf{H}}{\mathrm{N}_0})(\mathbf{I}+\frac{\mathbf{H}^\dagger\mathbf{H}}{\mathrm{N}_0}\kappa)^{-1})\right)}{\det\left(\mathrm{diag}(\mathbf{I}+\frac{\mathbf{H}^\dagger\mathbf{H}}{\mathrm{N}_0}\kappa)^{-1}\right)} d\kappa. \qquad (65)$$

To show that in low SNRs the iterative and non-iterative receivers have the same performance, we need to show that the function in the integral in (65) is a constant function $\kappa \in [0, 1]$. Then the result of the integral equals to the value of the function for $\kappa = 1$ which represents the achievable rate for a non-iterative MMSE receiver.

First note that the argument inside the integral in (62) and (65) is a monotonically decreasing function of parameter κ because the MMSE receiver increases the SINR when the variance of interference decreases. Thus, if we show that the values of the function for $\kappa = 0$ and $\kappa = 1$ are the same (or the ratio of these two values goes to one), we can conclude that the function is constant in the interval $[0, 1]$. The ratio is in the following form

$$\det(\mathrm{diag}(\mathbf{I} + \frac{\mathbf{H}^{\dagger}\mathbf{H}}{\mathrm{N}_0}))\det(\mathrm{diag}(\mathbf{I} + \frac{\mathbf{H}^{\dagger}\mathbf{H}}{\mathrm{N}_0})^{-1}). \tag{66}$$

As $\mathrm{N}_0 \to \infty$, (66) goes to one (the matrices approach identity $\mathbf{I}$), which completes the proof.

3.6 Numerical Results

We apply now the developed expressions to calculate the achievable rate in uncorrelated Rayleigh fading MIMO channels with $N = N_{\mathrm{t}} = N_{\mathrm{r}}$. In each scenario, the ergodic capacity C is obtained averaging $\mathrm{C}_{\mathbf{H}}$ over 2000 independent channel realizations with independent zero-mean entries so $\mathbb{E}\left\{\mathrm{tr}\left(\mathbf{H}\mathbf{H}^{\dagger}\right)\right\} = N$. Although we consider here one specific channel model, the method can be easily applied to any fading.

Figure 15 shows the achievable rate of MMSE non-iterative and iterative receiver where $N = 2, 4, 6$. We can observe that for high and low SNRs both curves converges as predicted by observation 2. Figure 16 shows the performance of

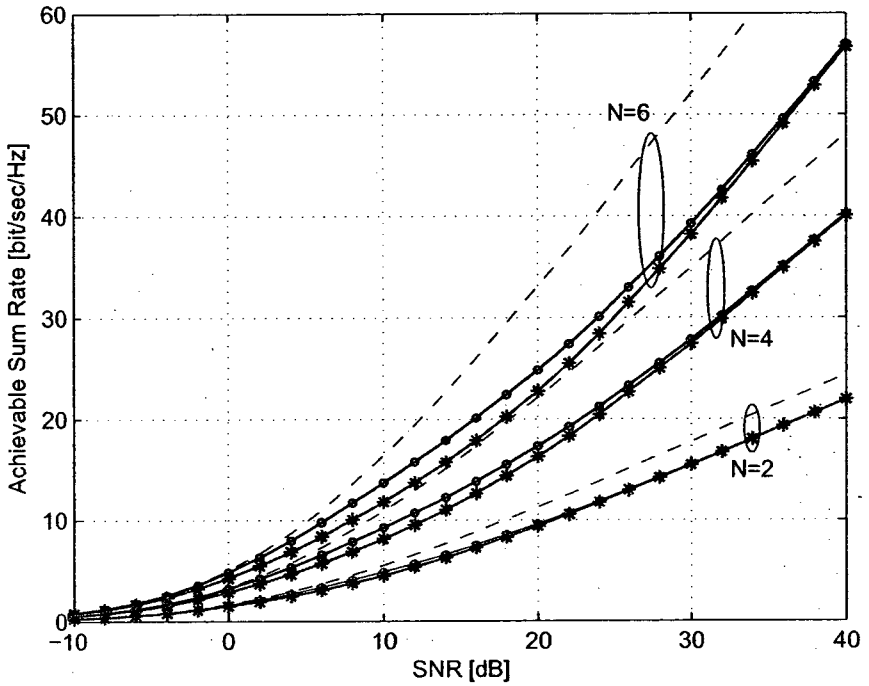

Figure 15: Achievable sum rate for a large-size QAM $N \times N$ uncorrelated Rayleigh fading MIMO channel for, a) non-iterative MMSE receiver (solid line with stars), b) iterative MMSE receivers (solid line with circles) and c) MIMO channel Shannon capacity (dashed line).

the MRC receiver where the gap between the iterative and non-iterative receivers is well appreciated. Unlike the MMSE receivers, the achievable rates by MRC receivers do not increase with SNR because the interference that is not mitigated for $\kappa = 1$ dominates its performance. Note that the results appearing in Fig. 15 slightly differ from those in Fig. 8 and those presented in [25] which considers the Gaussian constellation $\mathcal{X}$ while, here, we deal with uniform large-size QAM. Figure 17 compares the performance of MMSE and MRC in low SNR.

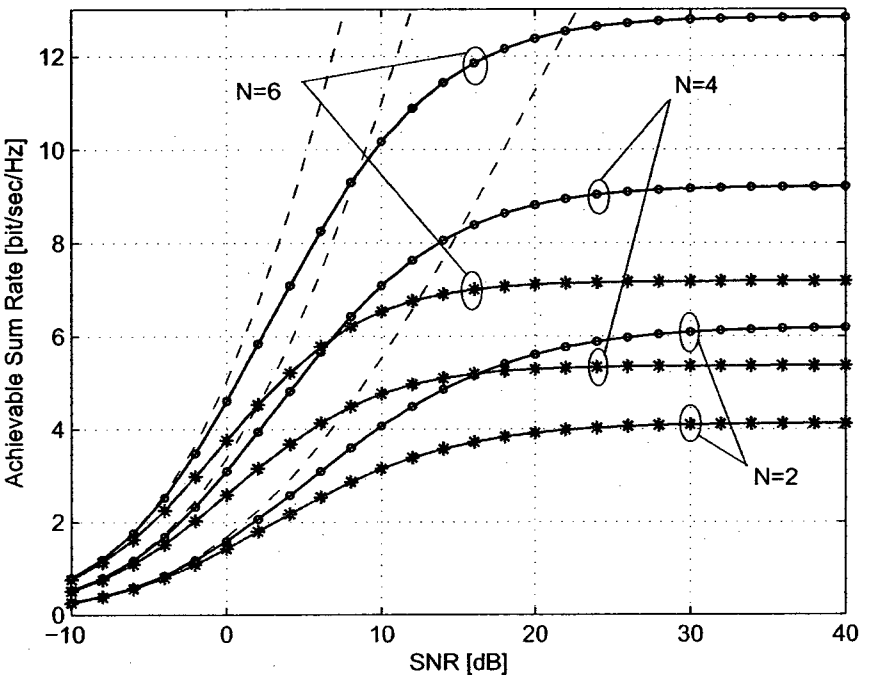

Figure 16: Achievable sum rate for a large-size QAM $N \times N$ uncorrelated Rayleigh fading MIMO channel for, a) non-iterative MRC receiver (solid line with stars), b) iterative MRC receivers (solid line with circles) and c) MIMO channel Shannon capacity (dashed line).

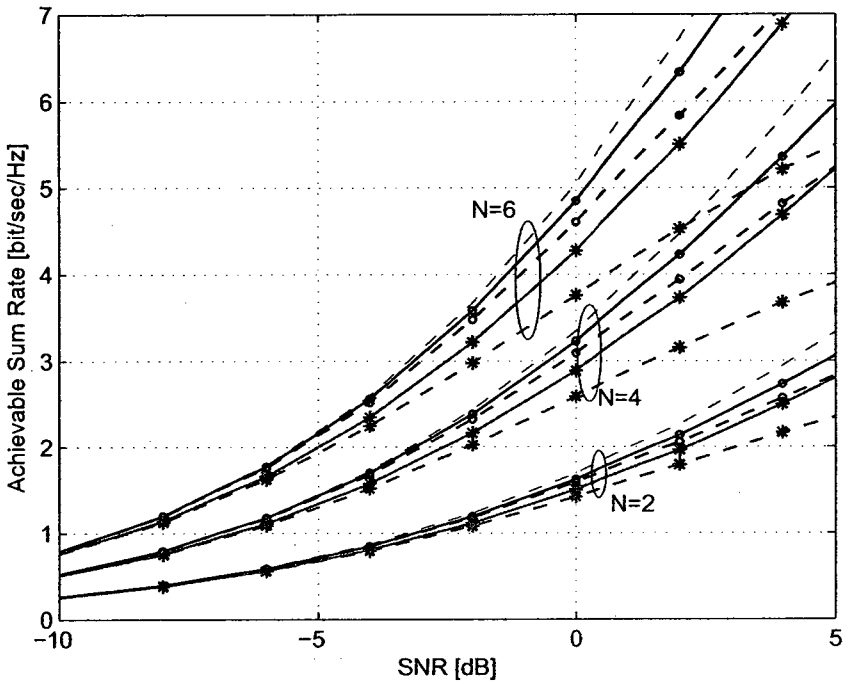

Figure 17: Achievable sum rate for $N \times N$ uncorrelated Rayleigh fading MIMO channel for, a) non-iterative MMSE receiver (solid line with stars), b) non-iterative MRC receiver (dashed line with stars), c) iterative MMSE receivers (solid line with circles), d) iterative MRC receivers (dashed line with circles) and e) MIMO channel Shannon capacity (dashed line).

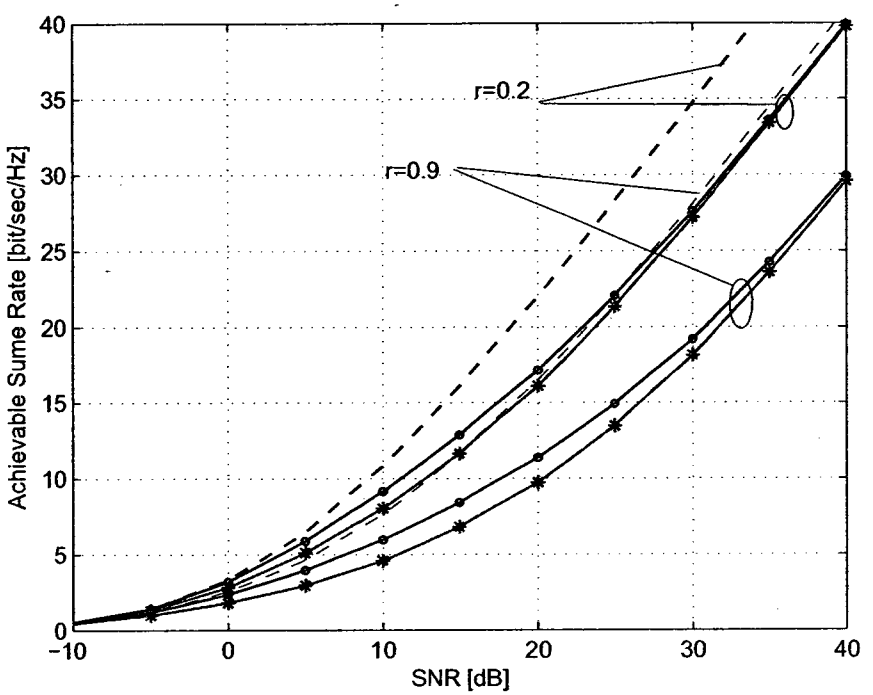

Figure 18: Achievable sum rate for 4×4 exponentially correlated fading MIMO channel with parameter r for, a) non-iterative MMSE receiver (solid line with stars), b) iterative MMSE receivers (solid line with circles) and c) MIMO channel Shannon capacity (dashed line).

A popular correlated fading model for MIMO channels is exponentially correlated fading with correlation matrix $\Sigma = \left\{r^{|i-j|}\right\}_{i,j=1,2,\ldots,N_r}$ and $r \in [0,1)$ [48]. In the Figure 18 and Figure 19 achievable sum rates of 4×4 MIMO channel which this fading model are plotted for $r = 0.2$ and $r = 0.9$ for receivers based on MMSE and MRC, respectively. Figure 20 also shows the achievable sum rate for $N \times N$ ($r = 0.9$)-exponential correlated fading MIMO channel for $N = 2, 4, 6$.

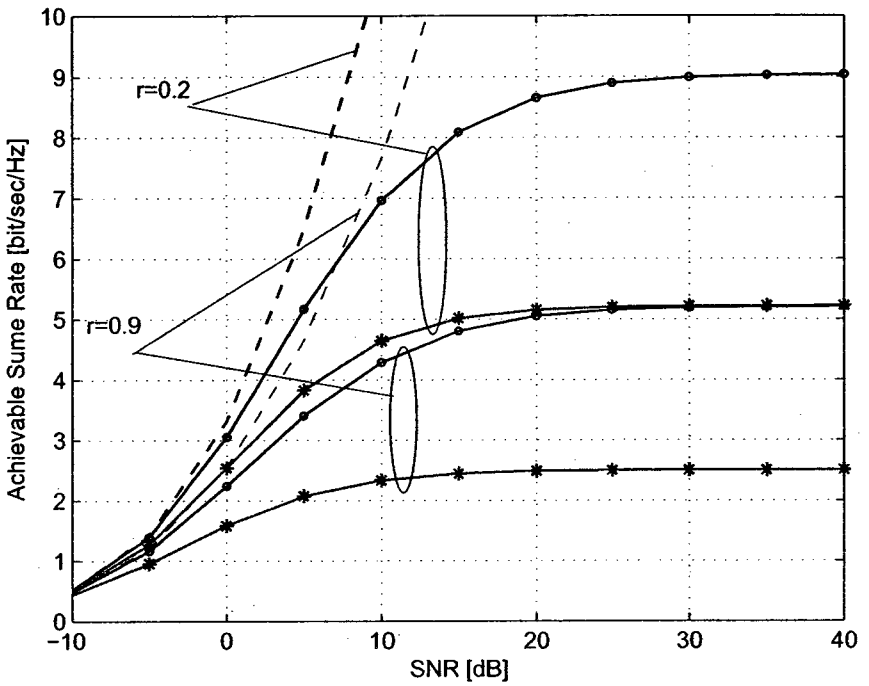

Figure 19: Achievable sum rate for 4×4 exponentially correlated fading MIMO channel with parameter r for, a) non-iterative MRC receiver (solid line with stars), b) iterative MRC receivers (solid line with circles) and c) MIMO channel Shannon capacity (dashed line).

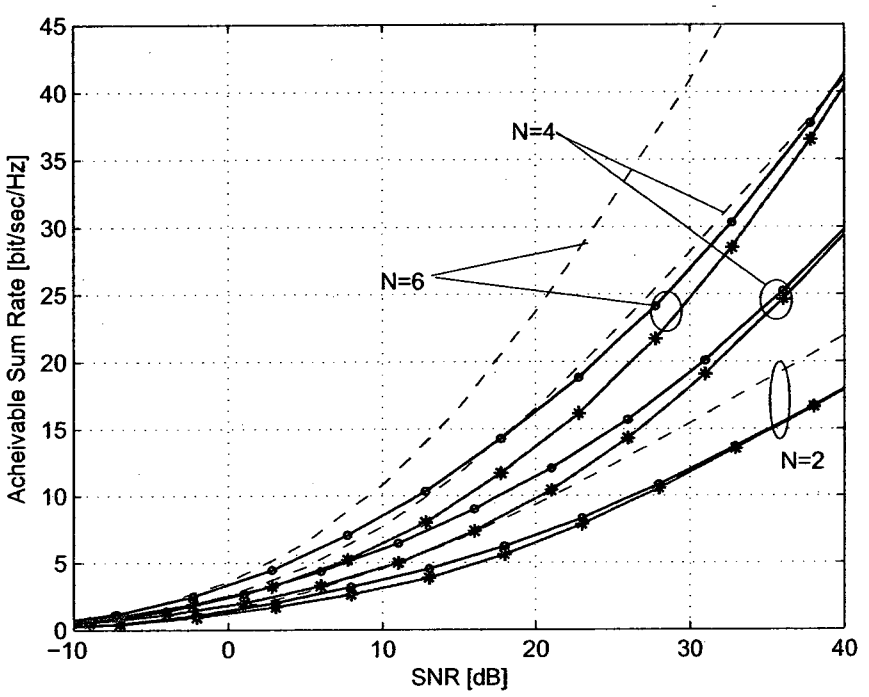

Figure 20: Achievable sum rate for $N \times N$ exponentially correlated fading MIMO channel with parameter $r = 0.9$ for, a) non-iterative MMSE receiver (solid line with stars), b) iterative MMSE receivers (solid line with circles), and c) MIMO channel Shannon capacity (dashed line).

3.7 Conclusion

In this work, we addressed the problem of finding the maximum achievable rates of iterative MIMO receivers with linear front-ends. We assumed an iterative receiver with two receiving modules (inner linear decoder and outer channel decoder) which exchange information between each other to achieve better performance. We assumed that the optimum channel decoder can be fit to the EXIT function of the linear detector and thus the achievable rate can be approximated as the area below the EXIT function of the detector. More practical cases with non-Gaussian signaling, where the information exchanged between the receiver's modules is in the form of LLRs (which is the case of common turbo receivers), were assumed and approximate achievable rates were derived. From the developed expressions, we concluded that for low and high SNR, iterative processing does not improve the MMSE receivers. In addition, we showed that, the achievable rates of the MRC-based receivers saturate at high SNRs and, for all range of SNRs, there is a considerable performance gap between the iterative and non-iterative cases, in favor of the former receiver. These conclusions were corroborated through several numerical examples.

Chapter 4

Sum-rate of single-user receivers

In this chapter, we derive expressions for the sum-rate of single-user receivers and we demonstrate their particular cases are known in the literature for minimum mean square error (MMSE) receivers in multiple-input multiple-output (MIMO) systems and for bit-interleaved coded modulation (BICM) transmission schemes.

4.1 Introduction

In this correspondence, applying the well-known chain-rule of mutual information between two vectors $\mathbf{x} = [x_1, \ldots, x_M]$ and $\mathbf{y} = [y_1, \ldots, y_N]$ [50, Ch. 2.5]

$$I(\mathbf{x};\mathbf{y}) = I(\mathbf{x}_{[i]};\mathbf{y}|x_i) + I(x_i;\mathbf{y}), \tag{67}$$

where $\mathbf{x}_{[i]}$ denotes $\mathbf{x}$ with x_i removed, we calculate the sum-rate of single-user (SU) receivers which, by definition, estimate x_i from $\mathbf{y}$ by marginalizing over

the unknown $\mathbf{x}_{[i]}$. As such, the achievable sum-rate is then given by the sum of mutual information $C^{\text{SU}} = \sum_i I(x_i; \mathbf{y})$. On the other hand, the multi-user (MU) receiver estimates jointly all the elements of $\mathbf{x}$, and therefore, its rate is given by $C^{\text{MU}} = I(\mathbf{x}; \mathbf{y})$.

We show that the sum-rate of SU receivers can be expressed as a combination of the rates of MU receivers. These conclusions are valid for any system (that is, for linear or non-linear relationship between $\mathbf{x}$ and $\mathbf{y}$) and for arbitrary distribution of $\mathbf{x}$. In light of this, the results reported in [51] and [25] can be considered as a special case since Gaussian $\mathbf{x}$ is assumed therein. Moreover, the approach we propose can be treated as an alternative simple proof of the results shown in [25].

Furthermore, the results for the bit-interleaved coded modulation (BICM) scheme presented in [49] are another instance of the general relationship we present and our derivation provides an alternative and very simple proof.

4.1.1 MIMO receivers

Consider a MIMO system employing M transmit and N receive antennas. Let $\mathbf{x}$ be the transmitted signal and $\mathbf{y}$ be the received signal, which are related as

$$\mathbf{y} = \mathbf{H}\mathbf{x} + \boldsymbol{\eta} = \sum_{i=1}^{n} \mathbf{h}_i x_i + \boldsymbol{\eta}, \tag{68}$$

where $\mathbf{H}$ is the $N \times M$ MIMO matrix and $\boldsymbol{\eta}$ is a noise vector.

Proposition 1 *The achievable sum rate of MIMO SU receivers can be expressed as*

$$C^{\mathrm{SU}}(\mathbf{H}) = M \cdot C^{\mathrm{MU}}(\mathbf{H}) - \sum_{i=1}^{M} C^{\mathrm{MU}}(\mathbf{H}_{[i]}), \tag{69}$$

where $\mathbf{H}_{[i]}$ *is the matrix* $\mathbf{H}$ *with the ith column removed.*

Proof. From (67), making explicit development of the expectation in conditional mutual information, we can write

$$I(x_i; \mathbf{y}) = I(\mathbf{x}; \mathbf{y}) - \sum_{z} I(\mathbf{x}_{[i]}; \mathbf{y} | x_i = z) \Pr(x_i = z) \tag{70}$$

$$= C^{\mathrm{MU}}(\mathbf{H}) - I(\mathbf{x}_{[i]}; \mathbf{y}_i') \tag{71}$$

$$= C^{\mathrm{MU}}(\mathbf{H}) - C^{\mathrm{MU}}(\mathbf{H}_{[i]}). \tag{72}$$

where $\mathbf{y}_i' = \mathbf{H}_{[i]}\mathbf{x}_{[i]} + \boldsymbol{\eta}$ is yielded, because knowledge of x_i in (70), lets us to eliminate its effect from y.

For continuous random variables x_i, the sum over the set of $\mathbf{x}_i = z$ in (70) should be replaced by integration. The sum-rate of SU receivers (69) is obtained by summing up the terms in (72).

By definition, the ergodic rate is obtained taking the expectation of the sum-rate $C^{\mathrm{SU}}(\mathbf{H})$ given by (69) with respect to $\mathbf{H}$, i.e., $C^{\mathrm{SU}}_{N \times M} = \mathbb{E}\{C^{\mathrm{SU}}(\mathbf{H})\}$, where the subindices denote the size of the MIMO matrix over which the averaging is carried out.

Proposition 2 *If all elements of the matrix* $\mathbf{H}$ *have the same distribution, and all elements of* $\mathbf{x}$ *have the same distribution, the ergodic sum rate can be expressed as*

$$C^{\mathrm{SU}}_{N\times M} = M \cdot \left(C^{\mathrm{MU}}_{N\times M} - C^{\mathrm{MU}}_{N\times(M-1)}\right), \tag{73}$$

Proof. Since the elements of $\mathbf{H}$ have the same distribution, averaging $C^{\mathrm{MU}}(\mathbf{H}_{[i]})$ is independent of i. That is, we can write $\mathbb{E}\{C^{\mathrm{MU}}(\mathbf{H}_{[i]})\} = C^{\mathrm{MU}}_{N\times(M-1)}$. Consequently, averaging (69) yields (73).

We emphasize that (69) and (73) are valid for $\mathbf{x}$ having an arbitrary distribution provided that the SU receiver applies optimal (i.e., maximum likelihood) detection. In case $\mathbf{x}$ contains discrete variables, exhaustive enumeration is required in the marginalization (over $\mathbf{x}_{[i]}$) and only for a particular case of Gaussian $\mathbf{x}$, the optimal detection boils down to a simple MMSE linear filtering, which is the case treated in [25]. Then, assuming that $\boldsymbol{\eta}$ is a zero-mean Gaussian vector with covariance matrix $\sigma^2_{\boldsymbol{\eta}}\mathbf{I}$ we can write

$$\begin{aligned} C^{\mathrm{SU}} = M \log_2 &\left(\det\left(\mathbf{I} + \frac{1}{\sigma^2_{\boldsymbol{\eta}}}\mathbf{H}\mathbf{H}^{\dagger}\right)\right) \\ &- \log_2\left(\prod_{i=1}^{M}\det\left(\mathbf{I} + \frac{1}{\sigma^2_{\boldsymbol{\eta}}}\mathbf{H}_{[i]}\mathbf{H}^{\dagger}_{[i]}\right)\right), \end{aligned} \tag{74}$$

where $(\cdot)^{\dagger}$ is the conjugate-transpose operator.

Considering power normalization, (74) is equivalent to the expressions shown in [25].

4.1.2 BICM Capacity

Consider now the general relationship between scalar y and the binary vector $\mathbf{x}$

$$y = \mu[\mathbf{x}] + \eta, \tag{75}$$

where $\mu[\cdot]$ is a bijective mapping of the binary vector onto constellation $\mathcal{X}$.

According to the principles of BICM transmission [52], the so-called BICM capacity[1]

$$\mathrm{C}_{\mathcal{X}}^{\mathrm{BICM}} = \sum_{i=1}^{N} I(x_i; \mathbf{y}), \tag{76}$$

defines the maximum transmission rate of a BICM system. Clearly, BICM capacity is the sum-rate when detecting the individual bit-streams x_i.

Proposition 3 *The BICM capacity can be expressed as [49]*

$$C_{\mathcal{X}}^{\mathrm{BICM}} = \sum_{i=1}^{M} \frac{1}{2} \sum_{b=0,1} (C_{\mathcal{X}}^{\mathrm{CM}} - C_{\mathcal{X}_{i,b}}^{\mathrm{CM}}) \tag{77}$$

where $C_{\mathcal{X}}^{\mathrm{CM}} = I(y; \mathbf{x})$ is the coded modulation rate defined in [53] for transmission with equiprobable symbols taken from the constellation $\mathcal{X}$, and $\mathcal{X}_{i,b} = \{z = \mu[x_1, \ldots, x_N] \in \mathcal{X} | x_i = b\}$ is a subset of the constellation $\mathcal{X}$ containing points whose labels $\mathbf{x}$ have the ith element set to b.

Proof. The proof can be found in [49], however, it may be simplified applying

[1] We continue to use the term "capacity" after [52] even if the distribution of $\mathbf{x}$ is not optimized.

(67) as follows:

$$I(y;x_i) = I(\mathbf{x};y) - I(\mathbf{x}_{[i]};y|x_i) \tag{78}$$

$$= I(\mathbf{x};y) - \sum_{b=0,1} I(\mathbf{x}_{[i]};\mathbf{y}|x_i=b)\Pr(x_i=b)$$

$$= \frac{1}{2}\sum_{b=0,1}\big(I(\mathbf{x};y) - I(\mathbf{x}_{[i]};y|x_i=b)\big). \tag{79}$$

Then, because $I(\mathbf{x}_{[i]};y|x_i=b) = C^{\mathrm{CM}}_{\mathcal{X}_{i,b}}$, summing (79) over i yields (77).

4.2 Conclusion

In this correspondence the sum-rate of SU receivers was expressed in terms of the rate of MU (joint) receivers and the simple proofs were provided by applying the well-known chain rule of mutual information.

Chapter 5

CFO-corrupted OFDM Systems Over Relay Channels

In this chapter, we analyze the impact of carrier frequency offset (CFO) on the performance of orthogonal frequency division multiplexing (OFDM) transmission employing space-frequency coding over relay channels. The challenge in such systems lies in the difficulty of cancelling the interference resulting from the different CFOs that correspond to the relays involved in the transmission. We first analyze the CFO correction schemes and examine their impact on the achievable information rates. Further, we analyze the interference cancellation (IC) technique based on the so-called turbo-principle, that is, which jointly detects and decodes the received data. The increase of the rates achievable thanks to IC is assessed via parametric description of the iterative process. We provide examples

that demonstrate the efficacy of the proposed scheme and numerical results are contrasted with theoretical performance limits.

5.1 Introduction

In this chapter with analyze the relay-based space-frequency coded OFDM transmission. We asses the rates achievable in the presence of the multiple CFOs and evaluate the potential of the rate increase due to iterative interference cancellation.

Cooperative transmission is considered a viable and low-cost solution to improve the coverage (reliability) of wireless communications [54]. In particular, the use of multiple relays that employ space time coding (STC) allow to harvest the diversity inherent in relay channels [55]. However, when employing STC, time synchronization between antennas becomes crucial [56]. To overcome this problem, one may use orthogonal frequency division multiplexing (OFDM), which has been adopted in many wireless communication standards including WiFi, WiMax [31], and LTE [30]. Since then, the code is constructed using space- and frequency-dimensions, such a scheme is called a space-frequency coding (SFC).

A downside of using OFDM is that it is sensitive to frequency synchronization errors [32] [57]. For instance, a slight carrier frequency offset (CFO) results

in destroying the orthogonality between subcarriers, leading to significant performance degradation. Therefore, accurate CFO estimation is essential to have a working OFDM system. The most common approach to the CFO-problem in single-antenna transmission relies on the accurate estimation of the CFO and its removal from the received signal through frequency correction [32] [59] [60]. On the other hand, in the case of multiple-relay transmission, the situation is similar to that occurring in orthogonal frequency division multiple access (OFDMA) where the base station receiver has to deal with CFOs that are different for various users [34]. The main difference with the single-user (or single relay) transmission is that the effect of CFO cannot be removed from the signal via simple frequency correction so interference is unavoidable.

Many papers had considered CFO estimation for OFDMA systems [34] [58] or methods to deal with the interference appearing in such cases [61] [62]. These works were based on the simulation of particular modulation/coding setups. Such an approach allows to validate basic concepts but makes it difficult to draw general conclusions, particularly when comparing different transmission strategies. Aiming at a more general results, we evaluate the transmission rates achievable for various strategies the receiver may deploy to mitigate the effects of the CFOs in relay-based SFC transmission. In particular, we assess the performance of the channel-dependent CFO correction and of an iterative (turbo) detection/decoding [63]. Our approach provides a picture that is more complete

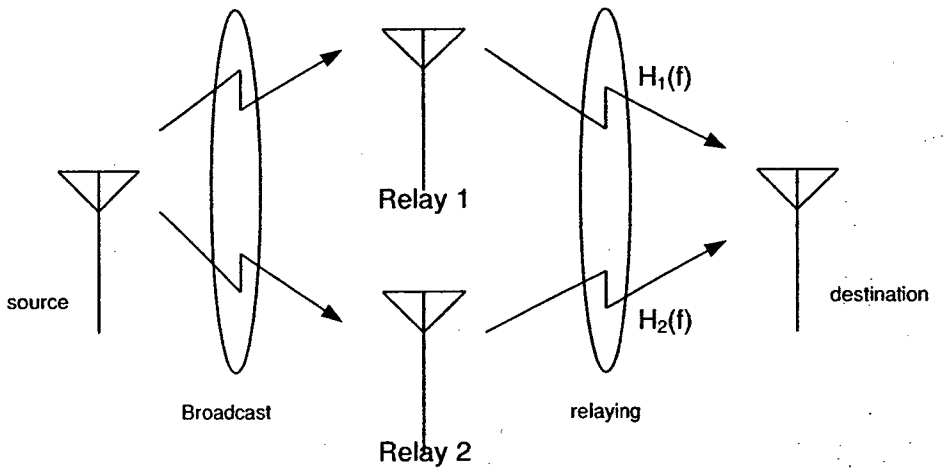

Figure 21: Model of a two-hop two-relay channel.

than any simulation-based study, can be related to particular cases of the coded transmission (that we also show as an example), and at the same time may be meaningfully contrasted with other relay-based transmission strategies.

The chapter is organized as follows: the system model is described in Sec. 5.2 and in Sec. 5.3 we analyze the throughput attainable with Alamouti SFC scheme in CFO-corrupted relay channel. The results obtained with practical coding/modulation schemes are presented in Sec. 5.4 and conclusions – in Sec. 5.5.

5.2 System model

We consider here a two-hop relay channel shown in Fig. 21, where the source terminal is broadcasting information toward the relays. Since the transmission is coded, the relays can reliably decode the broadcasted message and forward it to the destinations. We assume also that –in order to harvest the diversity of the relays-to-destination channels– the relays implement the Alamouti scheme [6]. This simplifies the receiver's processing as the sent symbols may be then recovered with a simple arithmetic operations.

In order to counteract –via simple processing– the effect of frequency-selective fading (on all links), we assume that the transmission is based on OFDM. This has the advantage of avoiding the strict time-synchronization requirement between the relays but its disadvantage is the sensitivity to the CFO at the destination. This problem of CFO in OFDM/OFDMA transmission has been extensively treated in the literature indicating the importance of accurate CFO estimation and correction, [34].

The Alamouti transmission scheme is thus affected by the interference due the residual CFO and its mitigation/reduction strategies are the main focus of this chapter.

To establish the notation, we consider the case of single-antenna OFDM

where N symbols $\mathbf{a} = [a_0, a_1, ..., a_{N-1}]^{\mathrm{T}}$ (we will use $(\cdot)^{\mathrm{T}}$ and $(\cdot)^{\mathrm{H}}$ to denote transpose and transpose-conjugate operators) are passed to a N-points inverse Discrete Fourier Transform (DFT). The resulting sequence is extended with the cyclic prefix, and sent over the frequency-selective channel whose frequency-reponse is known (i.e., accurately estimated). At the receiver, after sampling, and the prefix' removal, the signal is passed though the DFT which produces the signal

$$\mathbf{r} = \mathbf{F}\mathbf{D}(\delta)\mathbf{F}^{-1}\mathbf{H}\mathbf{a} + \mathbf{w} \tag{80}$$

where $\mathbf{r} = [r_0, r_1, ..., r_{N-1}]^{\mathrm{T}}$, $\mathbf{w} = [w_0, \ldots, w_{N-1}]^{\mathrm{T}}$ is a zero-mean Gaussian noise (AWGN) with autocorrelation $\mathrm{E}\{\mathbf{w}\mathbf{w}^{\mathrm{H}}\} = \mathbf{I}N_0$ ($\mathbf{I}$ is $N \times N$ identity matrix), $\mathbf{F}$ and $\mathbf{F}^{-1}$ are N-points DFT and inverse DFT matrices, $\mathbf{H} = \mathrm{diag}\{H_0, H_1, ..., H_{N-1}\}$ is the diagonal matrix whose entries are channel frequency responses $H_k = \sum_{n=0}^{N} h_n \exp(-2\pi kn/N)$ (where $h_n, n = 0, \ldots, N-1$ is the impulse response of the channel), and

$$\mathbf{D}(\delta) = \mathrm{diag}\left\{1, \mathrm{e}^{2\pi\delta/N}, \mathrm{e}^{2\pi\delta\cdot 2/N}, \ldots, \mathrm{e}^{2\pi\delta\cdot(N-1)/N}\right\} \tag{81}$$

is the diagonal matrix representing the effect of the CFO δ.

If $\delta = 0$, then $\mathbf{D}(\delta) = \mathbf{I}$ and (80) reduces to $\mathbf{r} = \mathbf{H}\mathbf{s} + \mathbf{w}$, otherwise symbols s_n interfere with each other, i.e., introduce the so-called inter carrier interference (ICI).

After some algebra it can be shown that [34]

$$r_n = H_n f(\delta) a_n + ICI_n(\delta) + w_n \tag{82}$$

where

$$f(\delta) = \frac{\sin(\pi\delta)}{N\sin(\frac{\pi\delta}{N})} e^{j\pi\delta\frac{N-1}{N}} \tag{83}$$

$$ICI_n(\delta) = \sum_{\substack{p=0 \\ p\neq n}}^{N-1} H_p a_p f(\delta + p - n) \tag{84}$$

We now extend the above model to the two-relay cooperative transmission scheme shown in Fig. 21. We are interested in the relay-destination communication, so we assume that the symbols $\mathbf{s} = [s_0, \ldots, s_{N-1}]^{\mathrm{T}}$ are received at the relays without errors. This is a reasonable assumption as we consider here a coded transmission. The symbols $\mathbf{s}$ are then forwarded towards the destination. Let $\mathbf{a}_i$ denote the sequence transmitted from the relay i ($i = 1, 2$). As such, the two sequences form a space-frequency code based on the Alamouti scheme. It can be expressed in a matrix form as

$$\mathbf{A} = \begin{bmatrix} \mathbf{a}_1^{\mathrm{T}} \\ \mathbf{a}_2^{\mathrm{T}} \end{bmatrix} = \begin{bmatrix} s_1 & -s_2^* & s_3 & -s_4^* & \cdots & s_{N-1} & -s_N^* \\ s_2 & s_1^* & s_4 & s_3^* & \cdots & s_N & s_{N-1}^* \end{bmatrix} \tag{85}$$

Consequently, the received signal after processing is in the following form

$$\begin{aligned} \mathbf{r} =& \mathbf{F}\cdot\mathbf{D}(\delta)\cdot\mathbf{F}^{-1}\cdot\mathbf{H}_1\cdot\mathbf{a}_1 + \\ & \mathbf{F}\cdot\mathbf{D}(\delta-\Delta)\cdot\mathbf{F}^{-1}\cdot\mathbf{H}_2\cdot\mathbf{a}_2 + \mathbf{w} \end{aligned} \tag{86}$$

where δ is the CFO between the destination and the first relay, Δ is the CFO between the second and the first relay, and $\mathbf{H}_i$, $i = 1, 2$ is the frequency responses of the channels between the i-th relay and the destination.

From (86) we see that, in general, no matter what strategy is chosen by the receiver for CFO compensation, some interference is unavoidable: it is possible to eliminate the effect of the CFO for the first relay ($\delta = 0$) or for the second one ($\delta = \Delta$), but the effect of both CFOs cannot be removed simultaneously (unless $\Delta = 0$, i.e., when there is no CFO between the relays).

Before considering any effect of the CFO-related interference, the receiver applies the conventional ST decoding to the received signals at time n and $n+1$ which have the following form [64], [65]

$$\begin{aligned} r_n =& H_{1,n} \cdot f(\delta) \cdot s_n + H_{2,n} \cdot f(\delta - \Delta) \cdot s_{n+1} + \\ & ICI_{1,n}(\delta) + ICI_{2,n}(\delta - \Delta) + w_n \end{aligned} \tag{87}$$

$$\begin{aligned} r_{n+1} =& - H_{1,n+1} \cdot f(\delta) \cdot s_{n+1}^* + H_{2,n+1} \cdot f(\delta - \Delta) \cdot s_n^* + \\ & ICI_{1,n+1}(\delta) + ICI_{2,n+1}(\delta - \Delta) + w_{n+1} \end{aligned} \tag{88}$$

The signals are gathered into a vector

$$\begin{aligned} \begin{bmatrix} r_n \\ r_{n+1}^* \end{bmatrix} =& \underbrace{\begin{bmatrix} H_{1,n} f(\delta) & H_{2,n} f(\delta - \Delta) \\ H_{2,n+1}^* f^*(\delta - \Delta) & -H_{1,n+1}^* f^*(\delta) \end{bmatrix}}_{\mathbf{B}_n} \begin{bmatrix} s_n \\ s_{n+1} \end{bmatrix} + \\ & \begin{bmatrix} ICI_{1,n}(\delta) + ICI_{2,n}(\delta - \Delta) \\ ICI_{1,n+1}^*(\delta) + ICI_{2,n+1}^*(\delta - \Delta) \end{bmatrix} + \begin{bmatrix} w_n \\ w_{n+1}^* \end{bmatrix}. \end{aligned} \tag{89}$$

and, next, the combining characteristic of the Alamouti scheme is applied

$$\begin{bmatrix} y_n \\ y_{n+1} \end{bmatrix} = \mathbf{B}_n^{\mathrm{H}} \begin{bmatrix} r_n \\ r_{n+1}^* \end{bmatrix} \tag{90}$$

Since all the transformations are linear, they may be written as

$$\mathbf{y} = \mathbf{G}\mathbf{s} + \mathbf{G}'\mathbf{s}^* + \mathbf{Q}\mathbf{w} \tag{91}$$

where the form of $\mathbf{G}$ and $\mathbf{G}'$ may be deduced from (84), (89) and (90). The matrix $\mathbf{Q}$ is block-diagonal composed of $\mathbf{B}_n^{\mathrm{H}}$ so the covariance of the noise-related term, given by $\mathsf{E}\{\mathbf{Q}\mathbf{Q}^{\mathrm{H}}\}N_0$ is also block diagonal with entires $\mathbf{B}_n^{\mathrm{H}}\mathbf{B}_n N_0$. If we assume that $H_{i,n} \approx H_{i,n+1}$, matrix $\mathbf{B}^{\mathrm{H}}$ is unitary, thus the covariance matrix' diagonal elements are given by $g_n = |H_{1,n}|^2|f(\delta)|^2 + |H_{2,n}|^2|f(\delta - \Delta)|^2$.

The observation $\overline{y}_n$ in (91) contains both the desired symbol $\overline{s}_n$ as well as its conjugate $\overline{s}_n^*$, and is affected by all other symbols and their conjugates (ICI). The detection is possible at this stage but, in the following we will use the symbols s_n are taken from the normalized constellation $\mathcal{Y}$ that is separable into identical real and imaginary parts, i.e., $\mathcal{Y} = \mathcal{X} \times (\jmath\mathcal{X})$. This happens, e.g., when M-ary quadrature amplitude modulation (M-QAM) is used. The constellation $\mathcal{Y}$ is zero-mean $\sum_{x\in\mathcal{Y}} x = 0$ and has unitary energy $E_{\mathcal{Y}} = \sum_{x\in\mathcal{Y}} |x|^2 = 1$, so the energy of the symbols $\overline{s}_n$ taken from $\mathcal{X}$ is $E_{\mathcal{X}} = \frac{1}{2}$.

Consequently, it is convenient to re-write (91) as

$$\overline{\mathbf{y}} = \begin{bmatrix} \mathbf{y}_R \\ \mathbf{y}_I \end{bmatrix} = \begin{bmatrix} \mathbf{G}_R + \mathbf{G}'_R & \mathbf{G}'_I - \mathbf{G}_I \\ \mathbf{G}_I + \mathbf{G}'_I & \mathbf{G}_R - \mathbf{G}'_R \end{bmatrix} \cdot \begin{bmatrix} \mathbf{s}_R \\ \mathbf{s}_I \end{bmatrix} + \begin{bmatrix} \mathbf{Q}_R & -\mathbf{Q}_I \\ \mathbf{Q}_I & \mathbf{Q}_R \end{bmatrix} \cdot \begin{bmatrix} \mathbf{w}_R \\ \mathbf{w}_I \end{bmatrix} \tag{92}$$

$$= \overline{\mathbf{G}}\overline{\mathbf{s}} + \overline{\mathbf{Q}}\overline{\mathbf{w}} \tag{93}$$

where $(\cdot)_R$ and $(\cdot)_I$ denote, respectively, the real and imaginary parts and $\overline{(\cdot)}$ denotes concatenation of the vectors/matrices appearing in (92).

5.3 Processing at the receiver

5.3.1 Perfomance Criterion

Since the receiver converts the signals $\overline{y}_n$ into reliability metrics that will be used by the channel decoder, it is relevant to use the mutual information (MI) between the metrics and the corresponding coded bits as the performance measure; it will provide us with information about the maximum achievable rate (or "constrained capacity") of the composite channel which comprises all the elements of the channel: modulation, DFT processing, and SF-decoding and that takes into account the CFO effects.

We assume that the interference can be approximated as Gaussian so the

signal-to-interference-and-noise ratio

$$\gamma_n = \frac{E_{\mathcal{X}} \cdot |\overline{g}_{n,n}|^2}{E_{\mathcal{X}} \cdot \sum_{l \neq n} |\overline{g}_{n,l}|^2 + \overline{q}_n \frac{1}{2} N_0} \quad n = 0, \ldots, 2N-1 \tag{94}$$

defines the mutual information for the n-th element of $\overline{\mathbf{y}}$ as $I_{\mathcal{X}}(\gamma_n)$, where the function $I_{\mathcal{X}}(\gamma)$ is acquired through numerical integration for a given $\mathcal{X}$ as explained in [52]. Here, $\overline{q}_n$ are the diagonal elements of $\overline{\mathbf{Q}}\,\overline{\mathbf{Q}}^{\mathbf{H}}$. If we assume that $\mathbf{B}_n$ are unitary, we can use $\overline{q}_{n+N} = \overline{q}_n \equiv |g_n|^2$ for $n = 0, \ldots, N-1$.

The estimate of the MI at the output of the receiver, providing information about the maximum attainable transmission rate is thus given by

$$I_{\text{tot}} = \frac{1}{N} \sum_{n=0}^{2N-1} I_{\mathcal{X}}(\gamma_n). \tag{95}$$

The maximum achievable rate I_{tot} is channel-dependent so to characterize the property of the transmission scheme in fading (variant) channel we will use the so called outage rate[1] $I_{\text{out},1-\epsilon}$ defined through

$$\Pr\{I_{\text{tot}} < I_{\text{out},1-\epsilon}\} = \epsilon. \tag{96}$$

This measure is convenient to evaluate the performance of the transmission over quasi-static channels, that is, where the coding and modulation are carried out in the same channel state (here: realizations of the channels' frequency responses $\mathbf{H}_1$ and $\mathbf{H}_2$). In fact, the outage rate is a much more practical measure

[1] It has the same meaning as the outage capacity, but the distinction is made to take into account the particular constellation $\mathcal{X}$.

that the so-called ergodic rate which requires the transmission to be sufficiently long to encompass all possible channel states.

In the following examples the channels between the relays and the destination are assumed to have two zero-mean circularly-symmetric, complex Gaussian, equal-power, independently fading taps, that is, $\mathsf{E}\{|h_0|^2\} = \mathsf{E}\{|h_1|^2\} = 0.5$. The number of sub-carriers is given by $N = 256$.

5.3.2 CFO Compensation

We are interested here in the effect of the CFOs δ and $\delta - \Delta$ on the capacity of the relay channel. First we analyze the impact of the selection of δ on the attainable rate I_{tot}.

In Fig. 22 we show I_{tot} as a function of δ for arbitrarily selected realization of channels $\mathbf{H}_1$ and $\mathbf{H}_2$. We also show the horizontal lines which denote the rate when only one relay (the first or the second) is used. In such a case, the CFO effect might be perfectly removed (that is why the capacity line is independent of δ) and, for a fair comparison with two-relay transmission, the transmission power from the transmitting relay is doubled.

The simplest strategy is to set $\delta = \frac{1}{2}\Delta$, so that, on average, both channels are affected in the same way. However, ignoring the knowledge of the channels $\mathbf{H}_1$ and $\mathbf{H}_2$ has a price: for example, if $\Delta = 0.6$, setting $\delta = \frac{1}{2}\Delta$ yields the rate $I_{\text{tot}} \approx 0.9$ while optimizing δ (setting $\delta = 0.1\Delta$) yields $I_{\text{tot}} \approx 1.2$.

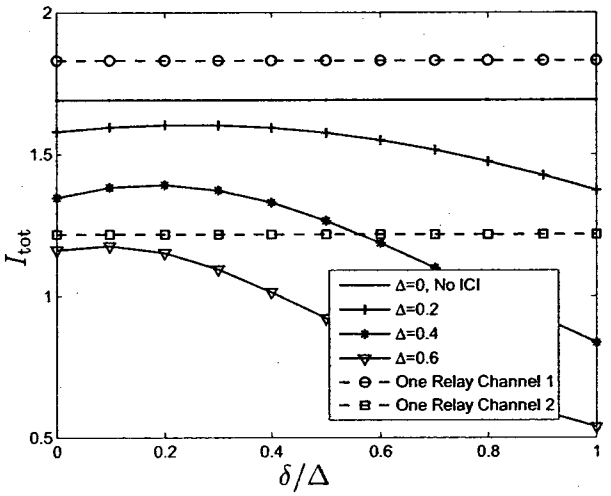

(a)

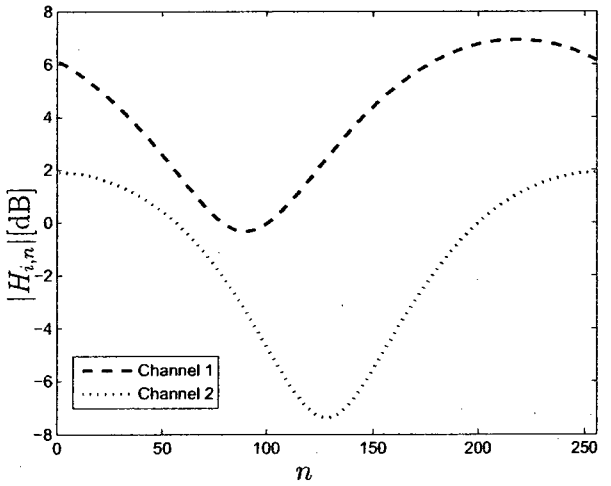

(b)

Figure 22: a) Relationship between I_{tot} and δ for channels $\mathbf{H}_1$ and $\mathbf{H}_2$ whose amplitude responses are shown in b); the transmission SNR $\frac{1}{N_0} = 8\text{dB}$.

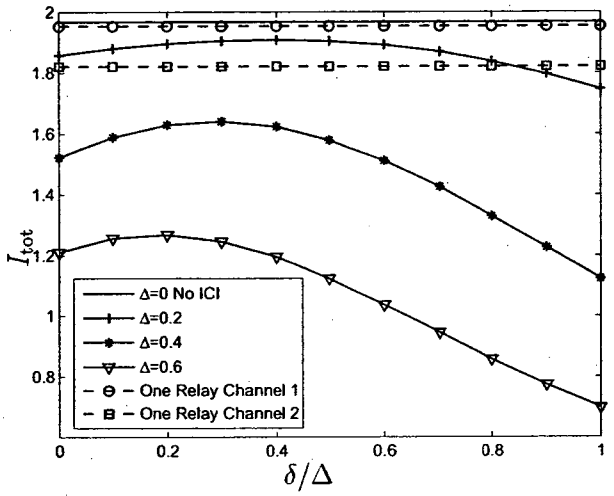

(a)

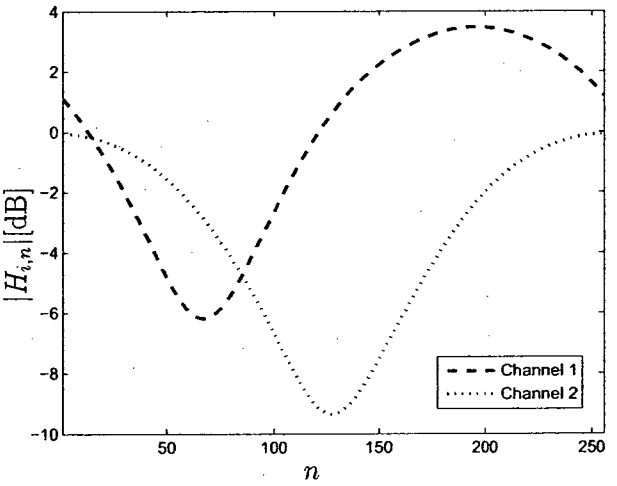

(b)

Figure 23: a) Relationship between I_{tot} and δ for channels $\mathbf{H_1}$ and $\mathbf{H_2}$ whose amplitude responses are shown in b); the transmission SNR is $\frac{1}{N_0} = 8\text{dB}$.

The case shown in Fig. 23 is slightly different as the optimized CFO ($\delta \approx 0.3\Delta$) would yield rates similar to $\delta = \frac{1}{2}\Delta$. The importance of the optimization of δ is elucidated further in Fig. 26 which gathers all the results.

5.3.3 Interference Cancellation (IC)

Up to now we assumed that the output of the ST combining is directly converted into reliability metrics. We note that the relationship (91) might be exploited to diminish the level of interference via linear, e.g., minimum mean-square error (MMSE), filtering of the output $\overline{\mathbf{y}}$. We let this option aside, nevertheless, it may be evaluated using the proposed methodology. Instead, we focus on the removal of interference using the information provided by the channel decoder as shown in Fig. 24.

If the decoder uses itself the iterative decoding, such an approach would not increase the processing complexity significantly, i.e., might be almost seamlessly included in the decoding process. On the other hand, linear filtering of $\overline{\mathbf{y}}$ would first require solving a $2N$-dimensional linear equation (to design the filter).

In practice, the decoder implements a soft-input soft-output processing which provides not only the estimates of the information bits but also the so-called extrinsic reliability metrics for all the coded (transmitted) bits b. These are usually expressed in the form of logarithmic likelihood ratios (LLR) $L = \log\big(\Pr(b=1)/\Pr(b=0)\big)$.

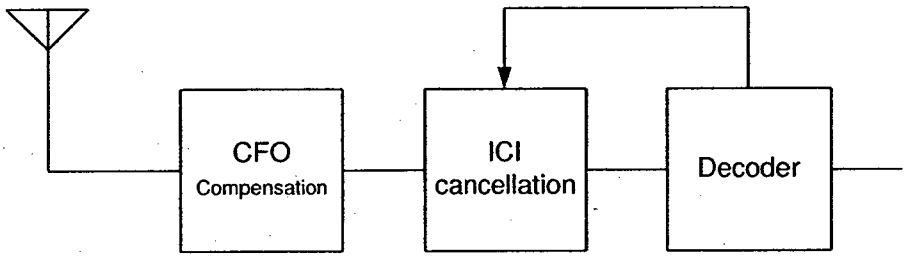

Figure 24: Model of the interaction between the decoder and the ICI cancellation: the decoder provides extrinsic LLRs that are used by IC.

The LLRs obtained from the channel decoder become a priori information which lets us to decrease the interference' energy. First, we calculate the expected values of the symbols

$$\hat{\bar{s}}_n = \mathrm{E}\{\bar{s}_n\} = \sum_{x \in \mathcal{X}} x \cdot \Pr(\bar{s}_n = x) \tag{97}$$

where $\Pr(x)$ are obtained from L as shown e.g. in [43].

Next, the effect of the symbols' estimates is substracted from the received signal

$$\bar{\mathbf{y}}' = \bar{\mathbf{y}} - (\overline{\mathbf{G}} - \mathrm{diag}(\overline{\mathbf{G}}))\hat{\bar{\mathbf{s}}} \tag{98}$$

which increases the effective SNR to

$$\gamma_n' = \frac{E_{\mathcal{X}} \cdot |\bar{g}_{n,n}|^2}{\sum_{l \neq n} |\bar{g}_{n,l}|^2 \cdot \mathrm{Var}\{\bar{s}_l\} + |\bar{g}_n|^2 \frac{1}{2} N_0} \tag{99}$$

where $\mathrm{Var}\{\bar{s}_n\} = \mathrm{E}\{(\bar{s}_n - \hat{\bar{s}}_n)^2\}$.

Since $\mathrm{Var}\{\overline{s}_n\} \leq E_{\mathcal{X}}$, $\gamma'_n \geq \gamma_n$.

5.3.4 Performance Limits of IC

In order to establish the limits of the proposed interference cancellation scheme, we rely on the parametric description of the iterative turbo process. Namely, we will use the so-called EXIT charts [20] to evaluate the achievable rates of the transmission. In particular, we will find the area below the EXIT function of the detector [22], which approximates well the maximum achievable transmission rate.

The EXIT function, characterizing the behavior of the detector in the iterative process, is obtained calculating the MI $I_{\mathrm{tot}} = I_{\mathrm{tot}}(I^{\mathrm{a}})$ as a function of a-priori MI I^{a} defined between the a priori reliability metrics L and the corresponding bits b. This is done as described in [20]: the metrics L are assumed to have Gaussian distribution with variance σ_L^2 and the mean $(b - \frac{1}{2}) \cdot \sigma_L^2$ conditioned on the bit's value b. In other words, L is treated as the outcome of a binary phase-shift keying (BPSK) transmission over AWGN channel with SNR defined as $SNR = \frac{1}{4}\sigma_L^2$, thus the a priori MI is given by

$$I^{\mathrm{a}} = I_{\mathrm{BPSK}}\left(\frac{1}{4}\sigma_L^2\right). \tag{100}$$

As conjectured by [22] the transmission rate for the receivers employing the

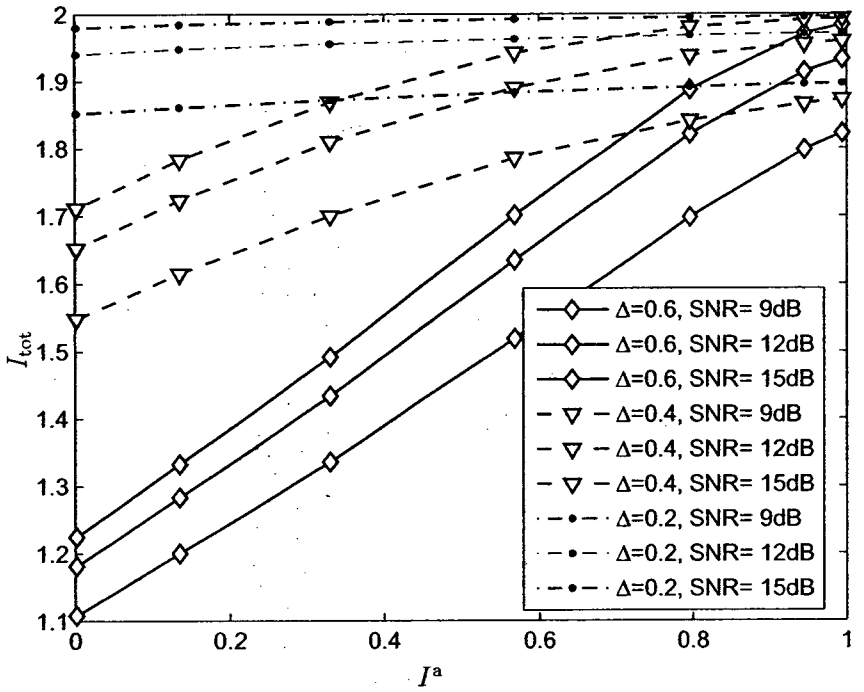

Figure 25: EXIT functions of the receiver for various values of Δ, and transmission SNR $SNR = \frac{1}{N_0}$.

iterative processing is bounded by the area below the EXIT function $I_{\text{tot}}(I^{\text{a}})$, i.e.

$$\tilde{I}_{\text{tot}} = \int_0^1 I_{\text{tot}}(I^{\text{a}}) dI^{\text{a}}. \tag{101}$$

Caution must be taken when using this interpretation of the area below the EXIT function as it is based on the assumption that the decoder's EXIT function is "matched" to the detector's function. That is, that both function do not cross each-other and the area between them is negligibly small. In practice, the decoder is channel-independent so some loss with respect to the predicted rate should be expected.

We note that, in general, the EXIT function may be obtained via numerical simulations, but here, we are able to deduce it knowing the relationship between I^{a} and $\mathrm{Var}\{s_n\}$. It can be found via numerical integration as shown in [43] and in a particular case of $\mathcal{X}$=BPSK we will consider here, the average variance of the symbols is given by

$$\overline{\mathrm{Var}}\{s\} = 1 - \int_{-\infty}^{\infty} \Phi(\lambda; \sigma_L^2) \cdot \tanh^2(0.5 \cdot \lambda)\, d\lambda \tag{102}$$

where $\Phi(\lambda; \sigma_L^2) = \frac{1}{\sqrt{2\pi}\sigma_L} \exp\left(-(\lambda - 0.5 \cdot \sigma_L^2)^2 / (2\sigma_L^2)\right)$.

Thus, the EXIT function may be obtained efficiently (without Monte-Carlo simulations) if we use (100) to relate σ_L^2 with I^{a}, apply (102), replace $\mathrm{Var}\{s_n\}$ with $\overline{\mathrm{Var}}\{s\}$ in (99), and use γ_n' instead of γ_n in (95).

Figure 25 shows the EXIT function $\tilde{I}_{\mathrm{tot}}(I^{\mathrm{a}})$ for a particular channel realization and different values of Δ, $\delta = \frac{1}{2}\Delta$, and $SNR = \frac{1}{N_0}$. The area (101) is then easily calculated. Note that the EXIT function, $I_{\mathrm{tot}}(0)$ corresponds to I_{tot} with "one-shot" detection, that is, when no iterative IC is employed. It is thus easy to observe that the improvement due to iterative IC when compared to non-iterative approach will be particularly important for large values of Δ (as expected because in such a case the interference is significant).

All the results are gathered in Fig. 26 where the outage rates $I_{\mathrm{out},0.99}$ and $\tilde{I}_{\mathrm{out},0.99}$ are shown for the CFO compensation explained in Sec. 5.3.2, with and without IC explained in Sec. 5.3.3. For comparison, we show the results of the

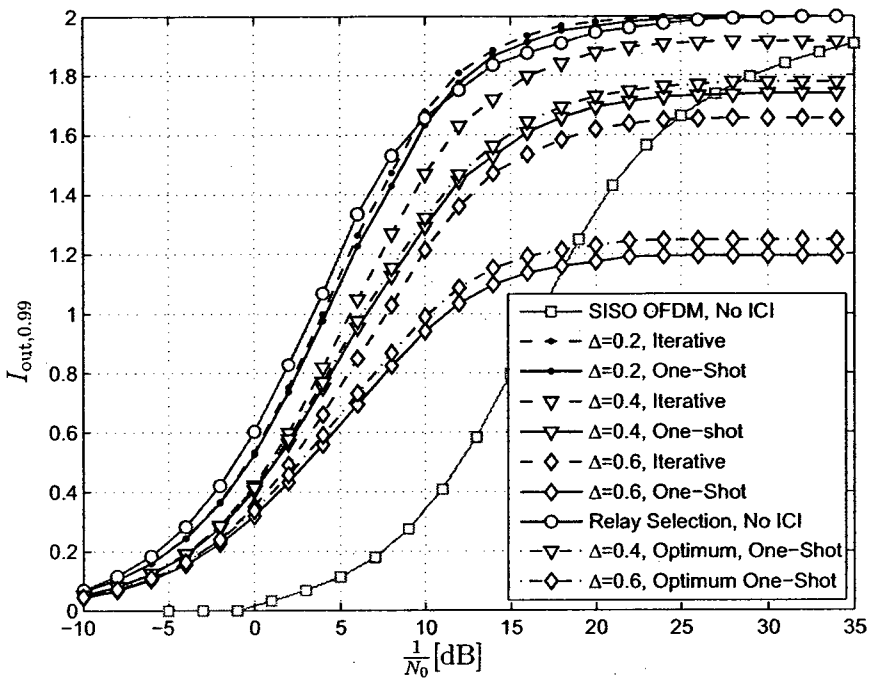

Figure 26: Outage rate ($\epsilon = 0.01$) versus transmission SNR $\frac{1}{N_0}$ for different processing schemes and $\mathcal{Y}$=4-QAM; "one-shot" detection means that IC is not used, while optimum "one-shot" means that δ was optimized.

single-relay transmission and the relay-selection results. The latter is feasible only if the receiver deciding which relay-transmission provides the largest rate, is capable of feeding this information back to the relays.

We may appreciate that the optimal selection of δ provides only a slight rate increase when comparing to that obtained setting $\delta = \frac{1}{2}\Delta$; this frees us from from doing this optimization at the receiver. On the other hand, the iterative IC may provide significant gains which, as expected, are particularly important with growing value of Δ. We note also that the achievable rate for $\Delta = 0.2$

is practically the same as in the case of relay-selection, independently whether IC is used or not. This is because with Alamouti SFC scheme, unlike in the case of relay-selection, we take also advantage of the frequency diversity, that is, amplitude-response of $\mathbf{H}_1$ and $\mathbf{H}_2$ is taken into consideration. As we saw on the example shown in Fig. 23, this may make the Alamouti scheme perform better than any of the relays taken individually.

5.4 Practical coded-modulation scheme

Finally, to illustrate the analysis we show an example of the coded transmission using 1360 information bits encoded with rate $\rho = \frac{2}{3}$ parallel concatenated convolutional codes (PCCC), i.e., turbo code, consisting of two identical component convolutional codes with generator $\{7, 5\}_8$. 4QAM modulation is used which corresponds to the target transmission rate of $I = 2\rho = 1.33$. The coded bits are modulated and sent over four OFDM blocks within which the channel is kept constant.

In Fig. 27, we show the bit error rate (BER) at the third iteration for two different values of Δ with and without the interference cancellation (IC). From Fig. 26 we may read that when $\Delta = 0.6$, the transmission rate $I = 1.33$ is not achievable with "one-shot" receiver but may be achieved when iterative IC is used. This is reflected in the simulation results as the BER curves tends to show

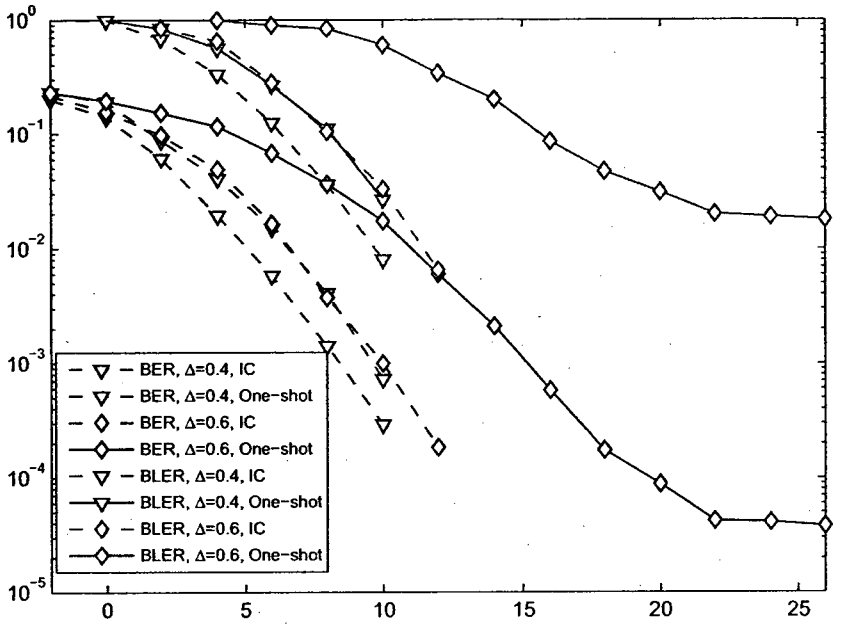

Figure 27: Bit- and block error rates (BER and BLER) versus transmission SNR for 4-QAM with and without interference cancellation at the receiver.

the error-floor with "one-shot" processing. On the other hand, iterative IC, yields the regular decrease of the BER/BLER when SNR increases.

According to Fig. 26, when $\Delta = 0.4$ the rate $I = 1.33$ may be achieved regardless of the processing employed but IC provides the SNR gain of roughly 2dB. A similar SNR-improvement is observed in the simulations.

5.5 Conclusion

In this Chapter, we analyzed the impact of carrier frequency offset (CFO) on the performance of orthogonal frequency division multiplexing (OFDM) transmission employing space-frequency coding over relay channels. From the point of view of achievable transmission rates, we evaluated the CFO correction schemes and assessed the gains obtained when the received is dotted with the interference cancellation (IC) based on the turbo-principle. For the two-tap model of the transmission channel we evaluate the outage of the two-relay Alamouti SFC scheme and compared it to a single-relay transmission. The results indicate that a) the channel-dependent CFO correction provides only marginal performance gain, b) despite severe CFO the relay-based transmission may provide significant diversity gains over one-relay transmission, and c) the performance may be significantly increased via iterative interference cancellation. The conclusions drawn from the proposed analysis were illustrated with numerical simulations.

Chapter 6

Conclusions and Future Work

6.1 Conclusions

In this thesis, we have presented an analytical framework for investigating the performance of iterative receivers, which attempt to iteratively mitigate the effect of interference. As a general example of interference communication, we focused on MIMO transmission. We concentrated on more practical receivers with linear front ends instead of optimal nonlinear and though complex ones, where well-known soft information about the transmitted bits in the form of LLRs are exchanged among the receiver's elements. Two types of linear combiner, MMSE and MRC, were discussed, however it is not hard to generalize the method for any linear combiner. In this approach the idea of area property in so-called EXIT

charts has been used for approximating the rates achievable by iterative processing and the method for derivation appropriate EXIT charts has been explained. It was shown that iterative MIMO receivers applying MMSE-base linear combiner shows the same performance in the sense of achievable rate as non-iterative receivers in low and high SNRs with large size QAM. The achievable rates as a function of SNR for MRC and MMSE based MIMO receivers for iterative and non iterative types were shown and compared for some fading channels and number of transmitters.

In addition, we developed the capacity of single user uplink MIMO using Chain rule of mutual information which relates it to the multiuser capacity and then, exploiting this general relation, the new more simple proofs for achievable sum rate of MIMO MMSE systems and BICM capacity were presented.

As an example of interference communication, the CFO corrupted cooperative system was discussed where the transmitter sends information to the receiver using Alamouti space-frequency coding in OFDM system through two relays. The effect of CFOs from each of the two paths, which is not possible to be completely canceled through the receiver's processing, were studied and achievable rates for different transmission and combining scenarios were shown.

6.2 Suggestions for Future Work

A few areas for further research and expansion of the presented work are shown below.

- In Chapter 3, while evaluating the achievable sum rates of MIMO receivers with iterative interference cancellation, we have assumed some simplifying, but not practical, assumptions. Considering these kinds of imperfections and evaluating their effects on the system performance and comparing the performance to the idealized system as the reference system can be viewed as interesting topics for further research. Some examples of these assumptions are described as follows.

  - We always have assumed that the receiver has the complete information about the channel state information (CSI) which is not exact knowing that practically the receiver always tries to estimate the channel and some estimation errors appears which basically depends on the fading model of the channel and estimation method exploited by the receiver. Thus, naturally, this question arise that: "For a specific fading model and estimation method, how much would the achievable rate change assuming the imperfection effect of channel estimation?". We should note that the achievable rate of this receiver model with iterative process where the receiver does not know CSI is another problem

and is still unsolved.

- In Chapter 3, the basic idea of calculation of the achievable rate of MIMO iterative receivers with linear front ends in uncorrelated Rayleigh fading channel, by relating that to the both correlated and uncorrelated Rayleigh fading MIMO capacity (as a special case for the materials presented Chapter 4), are presented. Continuing the introduced procedure to reach a closed form mathematical representation of this capacity for different fading channel models would be very interesting problem to solve in further works.

- In order to use the benefits of known gap between the channel capacity with Gaussian signaling and large-size constellation constrained capacity and assuming the fact that the Gaussian channel capacity can be calculated through the well known Shannon formula ($\log_2(1 + \mathrm{SNR})$), we have considered this signal constellation in our model. However one can extend the results for specific constellations (MQAM, MPSK ...) instead.

- The linear relationship between mutual information about the transmitted bits and the signal power (symbols' variances) shown to be valid for large size constellation with Gray labeling. The extension of the results for different labeling strategies (anti-Gray, etc.) and the

comparison of the results can be viewed as very good topic for further works.

- The method presented in Chapter 3 introduces a new approach for evaluating the performance of iterative MIMO receivers with linear front end for other more practical space time-coding scheme and perhaps can be used to explain some observations about the performance of such systems.

- The results of the system model presented in Chapter 5 can be extended in different ways. In this chapter we have assumed a very simple multi-path channel model and only two relays and in the receiver more complex and more efficient methods based on MMSE, MRC or ZF can be replace to the presented receiver structure can be assumed. Although this would be easily the generalization of the same presented method, comparison of the results would be very interesting. In addition, more complicated and near to optimum algorithms can be exploited by the receiver in CFO compensation. In other words, better strategy for choosing the frequency of the mixer in the receiver after estimating the CFOs of different paths (e.g. based on MMSE) will slightly improve the receiver's performance. Taking these algorithms into the account and quantifying this complexity versus performance trade-off seems to be a very interesting extension of this work and can be investigated in future works.

Bibliography

[1] İ. E. Telatar, "Capacity of multi-antenna Gaussian channels," *Europ. Trans. Commun.*, vol. 10, no. 6, pp. 585-595, Nov-Dec. 1999.

[2] G. J. Foschini and M. J. Gans, "On limits of wireless communications in a fading environment when using multiple antennas," *Wireless Pers. Commun.*, vol. 6, pp. 311-335, Mar. 1998.

[3] C. E. Shannon, "A mathematical theory of communication," *Bell System Technical Journal*, vol. 27, pp. 379-423 and 623-656, July and October, 1948.

[4] L. Zheng, D. Tse, "Diversity and multiplexing: a fundamental tradeoff in multiple-antenna channels," *IEEE Trans. Inform. Theory*, Vol. 49, No. 5, pp. 1073–1096, May 2003.

[5] A. Goldsmith , *Wireless Communication*, New York, USA: Cambridge University Press, 2005.

[6] S. M. Alamouti, "A simple transmit diversity technique for wireless communications," *IEEE Jour. Selec. Areas Commun.*, vol. 16, no. 8, pp. 1451–1458, Oct. 1998.

[7] V. Tarokh V, N. Seshadri, and A. R. Calderbank, "Space-time codes for high data rate wireless communication: performance criterion and code construction," *IEEE Trans. Inform. Theory,* vol. 44, no. 2, pp. 744–765, Mar. 1998.

[8] P. W. Wolniansky, G. J. Foschini, G. D. Golden, R. A. Valenzuela, "V-BLAST: an architecture for realizing very high data rates over the rich-scattering wireless channel," in *in Proc. ISSSE '98*, Sept-Oct. 1998, pp. 295–300.

[9] T. M. Duman, A. Ghrayeb , *Coding for MIMO communication systems*, Southern Gate, England: John Wiley & Sons, 2007.

[10] G. Foschini, "Layered space-time architecture for wireless communication in a fading environment when using multiple antennas," in *Bell Labs, Tech. J.,* vol. 1, no. 2, pp. 41–59, Autumn 1996.

[11] G. D. Forney. "Concatenated codes". in *Technical Report,* 37, MIT, 1966.

[12] J. P. Odenwalder, "Concatenated Reed-Solomon/Viterbi channel coding for advanced planetary mission: Analysis, Simulations and Tests," in *Linkabit Corporation,* Final Report on contract No 953866, Dec. 1974.

[13] C. Berrou, A. Glavieux, and P. Thitimajshima, "Near Shannon limit error correcting coding and decoding: Turbo codes," in *in Proc. IEEE Int. Conf. on Commun. (ICC)*, May 1993, pp. 1064-1070.

[14] S. Benedetto, D. Divsalar, G. Montorsi, and F. Pollard, "Serial concatenation of interleaved codes: Performance analysis design, and iterative decoding," *IEEE Trans. Inform. Theory,* vol. 44, pp. 909-926, May 1998.

[15] R. G. Gallagers "Low Density Parity Check Codes," *Monograph M.I.T. Press,*, 1963.

[16] D. J. C. MacKay and R. M. Neal, "Near Shannon limit performance of low-density parity-check codes," *Electron. Lett.*, vol. 32, pp. 1645-1646, Aug. 1996.

[17] C. Douillard, M. Jèzèquel, C. Berrou, A. Picart, P. Didier, and A. Glavieux, "Iterative correction of intersymbol interference: turbo equalization," in *Europ. Trans. Telecom.*, vol. 6, No. 5, pp. 507–511, Sept. 1995.

[18] H. V. Poor, "Turbo Multiuser Detection: An Overview", *IEEE 6th Symp. on Spread-Spectrum Tech. & Appli.*, NJIT, New Jersey, USA, Sep. 6–8, 2000.

[19] S. Haykin, M. Sellathurai, Y. de Jong, and T. Willink, "Turbo-MIMO for wireless communications," *IEEE Commun. Mag.*, vol. 42, no. 10, pp. 48–53 Oct. 2004.

[20] S. ten Brink, "Convergence behaviour of iteratively decoded parallel concatenated codes," *IEEE Trans. Commun.*, vol. 49, no. 10, pp. 1727-1737, Oct. 2001.

[21] H. E. Gamal and R. Hammons, "Analyzing the turbo decoder using the Gaussian approximation," *IEEE Trans. Inform. Theory,* vol. 47, no. 2, pp. 671686, Feb. 2001.

[22] A. Ashikhmin, G. Kramer, and S. ten Brink, "Extrinsic information transfer functions: model and erasure channel property," *IEEE Trans. Inform. Theory,* vol. 50, no. 11, pp. 2657-2673, Nov. 2004.

[23] C. Mèasson, A. Montanari, T. Richardson and R. Urbanke, "The generalized area theorem and some of its consequences," 2005, *submitted to IEEE Trans. Inform. Theory.*

[24] M. Tüchler, "Design of serially concatenated systems depending on the block length," *IEEE Trans. on Commun.*, vol. 52, no. 2, pp. 209–218, Feb. 2004.

[25] M. R. McKay, I. B. Collings and A. M. Tulino, "Achievable sum rate of MIMO MMSE receivers: a general analytic framework," 2009, *submitted to IEEE Trans. Inform. Theory.*

[26] C. Herzet, N. Noels, V. Lottici, H. Wymeersch, M. Luise, M. Moeneclaey and L. Vandendorpe,"Code-aided turbo synchronization," *Proc. of IEEE.*, vol. 95, No. 6, pp. 1255–1271, Jun. 2007.

[27] A. P. Dempster, N. M. Laird, and D. B. Rubin, "Maximum-likelihood from incomplete data via the EM algorithm," *J. Roy. Stat. Soc.*, vol. 39, no. 1, pp. 138, Jan. 1977.

[28] F. R. Kschischang, B. J. Frey, and H. A. Loeliger,"Factor graphs and the sum-product algorithm," *IEEE Trans. Inf. Theory.*, vol. 47, no. 2, pp. 498519, Feb. 2001.

[29] A. P. Worthen and W. E. Stark,"Unified design of iterative receivers using factor graphs," *IEEE Trans. Inf. Theory.*, vol. 47, no. 2, pp. 843849, Feb. 2001.

[30] M. C. Ng, M. Vijayaraghavan, N. Dave, Arvind, G. Raghavan, J. Hicks, "From WiFi to WiMAX: Techniques for high-level IP reuse across Different OFDM protocols," *63rd Vehicular Tech. Conference (VTC) 2006 Spring*, pp. 137–141, May 2006.

[31] E. Dahlman, H. Ekstrom, A. Furuskar, Y. Jading, J. Karlsson, M. Lundevall, S. Parkvall, "The 3G long-term evolution - radio interface concepts and performance evaluation," *5th IEEE/ACM Intern. Conf. on MEMOCODE 2007*, pp. 71–80, May/June 2007.

[32] M. Speth, S. A. Fechtel, G. Fock and H. Meyr, "Optimum receiver design for wireless broad-band systems using OFDM Part I," *IEEE Trans. Commun.*, vol. 47, no. 11, pp. 1668–1677, Nov. 1999.

[33] E. Chiavaccini and G. M. Vitetta, "Maximum likelihood frequency recovery for OFDM signals transmitted over multipath fading channels," *IEEE Trans. Commun.*, vol. 52, no. 2, pp. 244251, Feb. 2004. 1999.

[34] M. Morelli, C. Jay Kuo, M. O. Pun "Synchronization techniques for orthogonal frequency division multiple Access (OFDMA): A tutorial review," *Proc. of IEEE*, vol. 97, no. 7, pp. 1394–1427, July 2007.

[35] D. S. Shiu, G. J. Foschini, M. J. Gans, and J. M. Kahn, "Fading correlation and its effect on the capacity of multielement antenna systems," *IEEE Trans. Commun.*, vol. 48, pp. 502-513, Mar. 2000.

[36] M. Chiani, M. Z. Win and A. Zanella, "On the capacity of spatially correlated MIMO Rayleigh-fading channels," *IEEE Trans. Inform. Theory,*, Vol. 49, No. 10, Oct. 2003.

[37] H. Shin and J. H. Lee, "Capacity of multiple-antenna fading channels: spatial fading correlation, double scattering, and keyhole," *IEEE Trans. Inform. Theory*, Vol. 49, No. 10, pp. 2636-2647, Oct. 2003.

[38] S. K. Jayaweera and H. V. Poor, "On the capacity of multiple-antenna systems in Rician fading," *IEEE Trans. wireless Commun.*, Vol. 4, No. 3, pp. 1102–1111, May 2005.

[39] S. ten Brink and B. Hochwald, "Achieving near-capacity on a multiple antenna channel," *IEEE Trans. Commun.*, vol. 51, no. 3, pp. 389-399, Mar. 2003.

[40] M. Tüchler, R. Koetter, and A. C. Singer, "Turbo equalization: principles and new results," *IEEE Trans. Commun.*, vol. 50, no. 5, pp. 754-767, May 2002.

[41] P. D. Alexander, A. J. Grant, and M. C. Reed, "Iterative detection on code-division multiple-access with error control coding," in *Europ. Trans. Telecom.*, Vol. 9, No. 5, pp. 419-426, Sept.-Oct. 1998.

[42] A. Hedayat and A. Nosratinia, "Outage and diversity of linear receivers in flat-fading MIMO channels," *IEEE Trans. Signal Proc.*, vol. 55, no. 12, pp. 5868–5873, Dec. 2007.

[43] C. Hermosilla and L. Szczecinski, "Performance evaluation of linear turbo-receivers using analytical extrinsic information transfer functions," *EURASIP Journal on Applied Signal Processing,* pp. 892–905, May 2005.

[44] L. Szczecinski and D. Massicotte "Low complexity adaptation of MIMO MMSE receivers, implementation aspects," in *Globecom 2005*, 2005, St. Luis, USA, Nov. 2005.

[45] M. Kang and M. S. Alouini, "Capacity of MIMO Rician channels," *IEEE Wireless Commun.,* vol. 5, no. 1, pp. 112-122, Jan. 2006.

[46] F. W. Sun and H. C. A. van Tilborg, "Approaching capacity by equiprobable signaling on the Gaussian channel," *IEEE Trans. Inform. Theory,* vol. 39, no. 5, pp. 714–1416, Sep. 1993.

[47] A. Alvarado, H. Carrasco, and R. Feick, "On adaptive BICM with finite block-length and simplified metrics calculation," in IEEE Veh. Technol. Conf. 2006, VTC-2006, Fall, Sep. 2006.

[48] V. A. Aalo, "Performance of maximal-ratio diversity systems in a correlated Nakagami-fading environment," *IEEE Trans. on Commun.*, vol. 43, pp. 2360-2369, Aug. 1995.

[49] A. Martinez, A. Guillén i Fàbregas, and G. Caire, "Bit-interleaved coded modulation in the wideband regime," *IEEE Trans. Inf. Theory*, vol. 54, no. 12, pp. 5447–5455, Dec. 2008.

[50] T. Cover and J. Thomas, *Elements of Information Theory*, 2nd ed. New York, USA: John Wiley & Sons, 2006.

[51] M. R. McKay, I. B. Collings, and A. M. Tulino, "Exploiting connections between MIMO MMSE achievable rate and MIMO mutual information," in *Proc. IEEE Int. Conf. on Commun. (ICC)*, Dresden, Germany, Jun. 2009.

[52] G. Caire, G. Taricco, and E. Biglieri, "Bit-interleaved coded modulation," *IEEE Trans. Inf. Theory*, vol. 44, no. 3, pp. 927–946, May 1998.

[53] G. Ungerboeck, "Channel coding with multilevel/phase signals," *IEEE Trans. Inf. Theory*, vol. 28, no. 1, pp. 55–67, Jan. 1982.

[54] A. Sendonaris, E. Erkip, and B. Aazhang, "User cooperation diversity, Part I and Part II," *IEEE Trans. Commun.*, vol. 51, no. 11, pp. 1927–1948, Nov. 2003.

[55] J. N. Laneman, and G. W. Wornell, "Distributed space-time-coded protocols for exploiting cooperative diversity in wireless networks" *IEEE Trans. Inf. Theory.*, vol. 49, no. 10, pp. 2415–2425, Oct. 2003.

[56] X. Li, "Energy efficient wireless sensor networks with transmission diversity" *IEEE Electronics Lett.*, vol. 39, no. 24, pp. 1753–1755, Nov 2003.

[57] T. Pollet, M. Van Bladed, and M. Moeneclaey, "BER sensitivity of OFDM systems to carrier frequency offset and Wiener phase noise," *IEEE Trans. Commun.*, vol. 43, no. 2/3/4, pp. 191–193, Feb., Mar., Apr. 1995.

[58] X. N. Zeng and A. Ghrayeb, "Joint CFO and channel estimation for uplink OFDM systems: An application the variable projection method," *IEEE Trans. Wireless Commun.*, vol. 8, no. 5, pp. 2306–2311, May 2009.

[59] X. N. Zeng and A. Ghrayeb, "A blind carrier frequency offset estimation scheme for OFDM systems with constant modulus signaling," *IEEE Trans. Commun.*, vol. 56, no. 7, pp. 1032-1037, July 2008.

[60] X. N. Zeng and A. Ghrayeb, "CFO estimation for differential OFDM systems," *IEEE Trans. Wireless Commun.*, vol. 8, no. 1, pp. 124-129, January 2009.

[61] M. Huang, X. Chen, S. Zhou and J. Wang, "Analysis of iterative ICI cancellation algorithm for uplink OFDMA Systems with carrier-frequency offset," *IEICE Trans. Commun.*, E90-B(7), pp. 1734–1745, 2007.

[62] T. Yucek and H. Arslan, "Carrier frequency offset compensation with successive cancellation in uplink OFDMA systems," *IEEE Trans. Wireless Commun.*, vol. 6, no. 10, pp. 1–6, Oct. 2007.

[63] Y. Miyauchi and T. Saba, "Turbo Equalization Combined Timing and Frequency Offsets Compensation in Uplink OFDMA Systems," *GLOBECOM'06*, pp. 1–5, Nov. 27-Dec. 1, 2006.

[64] S. Wu and Y. Bar-Ness, "OFDM systems in the presence of phase noise: conseguence and solutions," *IEEE Trans. Commun.*, vol. 52, no. 11, pp. 1988–1996, Nov. 2004.

[65] P. H. Moose, "A technique for orthogonal frequency division multiplexing frequency offset correction," *IEEE Trans. Commun.*, vol. 42, no. 10, pp. 2908–2914, Oct. 1994.